A Review of the Experimental Estimation of the Rotor Dynamic Parameters of Seals

R. Tiwari, S. Manikandan and S.K. Dwivedy

ABSTRACT—In this paper, we present a critical review of the experimental estimation of the rotor dynamic parameters (RDPs) of different types of seals. The main focus is on rotary seals for high-speed and high-pressure applications. These play an active role between the rotating and stationary parts of turbomachinery to prevent working fluid leakage; however, they can cause rotor instability. The main parameters that govern the instability are the RDPs of seals. This review includes a variety of rotary seals, a description of experimental rigs and measurement techniques, parameter estimation procedures, and uncertainty analysis. Based on the state of the art in the experimental estimation of the RDPs of seals, conclusions are made and future directions are suggested.

KEYWORDS: seals, rotor dynamic parameters, estimation procedures, error analysis

1. Introduction

Seals are mainly used to reduce the leakage of working and lubricating fluids through the interface between machine parts. Some leakage is inevitable, and it results in axial fluid velocities though the seal in the direction of the pressure drop. The present-day requirements of critical sealing applications have a diverse range of operating condition requirements, such as (i) cryogenic temperature, (ii) hard vacuum, (iii) ultra-clean systems, (iv) leakage control to 10^{-12} cc s^{-1}, (v) pressures over 100 bar, (vi) temperatures exceeding 800°C, (vii) hard-to-handle liquids and gases, (viii) high pressure pulsations, and (ix) rotor speeds as high as 10^5 rpm. These extreme conditions of seals are challenging tasks in the space age aviation and aerospace industries.

The importance of calculations of rotor dynamic parameters (RDPs)—rotordynamic (or dynamic) parameters are also known as: seals force (or moment) coefficients; added-mass, damping and stiffness coefficients; linearized rotordynamic parameters; dynamic impedances—of seals arose in the late 1970s with regard to instability problems within the operating speed range of compressors used in many industries and vibration problems related to high-pressure oxygen turbopump of the space shuttle main engine. Seals in the high-speed operations of turbomachines lead to instability. The main factor that governs the instability is the RDPs of seals. Although the importance of seal RDPs is generally well recognized by the design engineer, it is often the case that theoretical models available for predicting it are accurate for very specific cases. Moreover, RDPs of seals are greatly dependent on many physical and mechanical parameters, such as lubricant and working fluid temperatures, pressure drop, seal clearances, surface roughness and patterns, rotor speeds, eccentricity, and misalignments, and these are difficult to obtain accurately in actual test conditions. It is for this reason that designers of high-speed rotating machinery prefer experimentally estimated values of RDPs of seals in their calculations.

In this paper, a review has been made of the experimental estimation methods of RDPs of seals with the main focus on rotary seals. Table 1 contains a chronological list of source material, with brief details, on the experimental estimation of the RDPs of seals.

1.1. Classification of Seals

Seals are broadly classified as liquid and gas seals according to the working fluid used in the system. The most common working fluids are water, air, nitrogen, triflurobromomethane ($CBrF_3$), liquid oxygen, liquid hydrogen, etc. In addition, they can be categorized as static and dynamic seals. Static seals are used where the two surfaces do not move relative to one another. Gasket-type seals are static seals (Figure 1). Dynamic seals are used where sealing takes

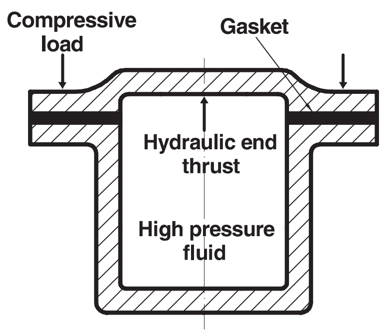

Figure 1. Static seal (gasket).

R. Tiwari (rtiwari@iitg.ernet.in), S. Manikandan and S.K. Dwivedy, Department of Mechanical Engineering, Indian Institute of Technology Guwahati, North Guwahati, Guwahati, 781039, India

The Shock and Vibration Digest, Vol. 37, No. 4, July 2005 261–284

DOI: 10.1177/0583102405055442

Table 1. A chronological summary of the literature on the experimental estimation of the RDPs of seals.

Reference	Type of seals, working fluids and applications	Seal dimensions (mm, wherever applicable)	Speeds (rpm), Reynolds numbers, pressures and pressure differences (bar)	Transducers, exciters and type of excitations (parameter estimation domain)	Parameters estimated (uncertainty analysis)
Black and Jenssen (1969/70)	PAS*, Water, Centrifugal pumps.	L/D = 0.25, 0.5 and 1, D = 50.8, C = 0.272	ω = 8000, R_a = 6000 – 20000, P = 17.2.	Disp. transducers, Unbalance: Sinusoidal. (Time)	Stiffness (UNR)
Falco et al. (1984)	PAS, Water, Centrifugal pumps.	L/D = 0.25, 0.75 and 1.25, D = 160, C = 0.18.	ω = 750 to 5000, ΔP = 10 – 35.	Disp. transducers, Hydraulic shaker: Sinusoidal. (Freq.)	Stiffness and damping (UNR)
Nordmann and Massmann (1984)	PAS, Water, Turbopumps.	L/D = 1.667, D = 21, C = 0.35.	ω = 6000, R_a = 10530, R_w = 2887, ΔP = 2.23.	Disp. transducers (Inductive), Impact hammer: Impulsive. (Freq.)	Mass, stiffness and damping (UNR)
Kanki and Kawakami (1984)	PAS and SS, Water, Centrifugal pumps.	L/D = 0.2 and 1, D = 200, C = 0.5	ω = 2000, ΔP = 10.	Disp. transducers, Hydraulic shaker: Sinusoidal. (Freq.)	Mass, stiffness and damping (UNR)
Childs and Kim (1985)	HDS and DDS $CBrF_3$, HPOTP.	L/D = 0.491 D = 101.6, C = 0.527.	ω = 7500, ΔP = 20.	Disp. transducers (capacitance) and pressure transducers (strain gage). Eccentric rotor. (Freq.)	Mass, stiffness and damping (UNR)
Childs and Dressman (1985)	TPAS, Water, Centrifugal pumps.	L/D = NA, D = 101.6, C = 0.508 (in) and 1.126 (out).	ω = 4152, ΔP = 10.	Disp. transducers (capacitance) and pressure transducers (strain gage). Eccentric rotor. (Freq.)	Stiffness and damping (UNR)
Childs et al. (1986)	PAS, HS and LS, Air, HPOTP.	L/D = 0.327, D = 152.8, C = NA.	ω = 8000, P = 7.7.	Disp. transducers (eddy-current), accelerometers and quartz load cells. Hydraulic shaker: Sinusoidal. (Freq.)	Stiffness and damping (UNR)
Nelson et al. (1986)	TPAS, Air, Compressors.	L/D = 0.333, D = 240, C (in) = 0.737 and 1.114, C (exit) = 0.737.	ω = 200 – 8000, P = 1.7 – 7.2.	Disp. transducers (eddy-current), accelerometers and quartz load cells. Hydraulic shaker: Sinusoidal. (Freq.)	Stiffness and damping (UNR)
Childs and Kim (1986)	RDS, $CBrF_3$, Turbopumps.	L/D = 0.491, D = 101.6, C = 0.527, h = 0.102.	ω = 7600, ΔP = 25.	Disp. transducers (capacitance) and pressure transducers (strain gage). Eccentric rotor. (Freq.)	Mass, stiffness, and damping. (UNR)
Childs and Scharrer (1986)	LS (TOS and TOR), Air, Turbopumps.	L/D = 0.336, D = 151.36, C = 0.406, h = 3.175.	ω = 8000, P = 8.25.	Disp. transducers (eddy-current), accelerometers and quartz load cells. Hydraulic shaker: Sinusoidal. (Freq.)	Stiffness, damping and uncertainty.
Childs and Garcia (1987)	SDS, $CBrF_3$, Turbopumps.	L/D = 0.491, D = 101.6, C = 0.527.	ω = 7600, ΔP = 25.	Disp. transducers (capacitance) and pressure transducers (strain gage). Eccentric rotor. (Freq.)	Mass, stiffness and damping. (UNR)
Childs and Scharrer (1988)	LS (TOS and TOR), Air, Turbopumps.	L/D = 0.35 and 0.336, D = 145 and 151.36, C = 0.3, 0.33, 0.4, 0.5 and 0.55, h = 3.175.	ω = 16000, P = 8.22.	Disp. transducers, accelerometers and quartz load cells. Hydraulic shaker: Sinusoidal. (Freq.)	Stiffness, damping and uncertainty.
Hawkins et al. (1989)	LR/HS, Air, Turbopumps.	L/D = 0.35, D = 145, C = 0.203, 0.304 and 0.406.	ω = 16000, P = 8.22.	Disp. transducers, accelerometers and quartz load cells. Hydraulic shaker: Sinusoidal. (Freq.)	Stiffness, damping and uncertainty.

Table 1. A chronological summary of the literature on the experimental estimation of the RDPs of seals.

Reference	Type of seals, working fluids and applications	Seal dimensions (mm, wherever applicable)	Speeds (rpm), Reynolds numbers, pressures and pressure differences (bar)	Transducers, exciters and type of excitations (parameter estimation domain)	Parameters estimated (uncertainty analysis)
Childs et al. (1989)	HS, LS and PAS, Air, HPOTP.	$L/D = 0.336$, $D = 151.36$, $C = 0.41$, h = 0.74,1.47 and 1.91, $d = 0.51$,0.79 and 1.57.	$\omega = 16000$, $P = 8.2$.	Disp. transducers, accelerometers and quartz load cells. Hydraulic shaker: Sinusoidal. (Freq.)	Stiffness, damping and uncertainty.
Elrod et al. (1989)	HS/SR, Air, Turbopumps.	$L/D = 0.336$, $D = 151.36$, $C = 0.41$, $h = 1.47$ and 1.91, $d = 0.51$ and 1.57.	$\omega = 16000$, $P = 8.2$.	Disp. transducers, accelerometers and quartz load cells. Hydraulic shaker: Sinusoidal. (Freq.)	Stiffness and damping. (UNR)
Childs et al. (1990a)	HS, Air, Turbomachinery.	$L/D = 0.168$, $D = 302.8$, $C = 0.41$, $h = 3.18$, $w = 1.59$, 0.793 and 0.508.	$\omega = 16000$, $P = 18.3$.	Disp. transducers, accelerometers and quartz load cells. Hydraulic shaker: SSW. (Freq.)	Stiffness, damping and Uncertainty
Childs et al. (1990b)	HGS/SR, $CBrF_3$, Turbomachinery.	$L/D = 0.5$, $D = 101.6$, $C = 0.37$, $\alpha = 0 - 70$.	$\omega = 7200$, $P = 40$.	Disp. transducers (capacitance) and pressure transducers (strain gage). Eccentric rotor. (Freq.)	Stiffness and damping. (UNR)
Childs et al. (1990c)	RDS, $CBrF_3$, Turbomachinery.	$L/D = 0.5$, $D = 102$, $C = 0.38$.	$\omega = 7500$, $R_a = (9 \text{ to } 25) \times 10^4$, $\Delta P = 40$.	Disp. transducers (capacitance) and pressure transducers (strain gage). Eccentric rotor. (Freq.)	Stiffness and damping. (UNR)
Iwatsubo et al. (1990)	TDS, Water, Centrifugal pumps.	$L/D = 0.5$, $D = 70.35$, $C = 0.175$, $h = 0.5$ and 0.3.	$\omega = 500 - 4500$, $\Delta P = 294 - 8.82$.	Disp. transducers, pressure transducers and piezoelectric load cells. Eccentric sleeves. (Freq.)	Stiffness and damping. (UNR)
Childs and Ramsey (1991)	LR/HS with and without SB, Air, HPFTP.	L/D = NA, $D = 146.15$, $C = 0.31$.	$\omega = 16000$, $P = 18.3$.	Disp. transducers, accelerometers and quartz load cells. Hydraulic shaker: SSW. (Freq.)	Stiffness, damping and uncertainty.
Childs et al. (1991)	HS with SB, Air, HPOTP.	$L/D = 0.172$, $D = 146.15$, C = NA, $w = 1.40$, $h = 3.81$.	$\omega = 16000$, $P = 18.3$.	Disp. transducers, accelerometers and quartz load cells. Hydraulic shaker: SSW. (Freq.)	Stiffness, damping and uncertainty.
Childs and Kleynhans (1992)	HS, PAS and LS, Air, HPOTP.	$L/D = 1/6$, $D = 152.4$, $C = 0.30$.	$\omega = 16000$, $P = 18.3$ bar.	Disp. transducers, accelerometers and quartz load cells. Hydraulic shaker: SSW. (Freq.)	Stiffness, damping and uncertainty.
Kanemori and Iwatsubo (1992)	LPAS, Water, Centrifugal pumps.	$L/D = 3$, $D = 80$, $C = 0.394$	$\omega = 3000$, $P = 15$.	Disp. transducers (eddy-current), pressure transducers (strain-gage) and piezoelectric load cells. Eccentric sleeves. (Freq.)	Mass, stiffness, damping, moment coefficients and uncertainty.
Brown and Ismail (1992)	LPAS, Water, Centrifugal pumps.	$L/D = 0.995$, $D = 100.5$, $C = 0.25$	$\omega = 1600$, $\Delta P = 15.7$.	Disp. transducers, accelerometers and load cells. Hydraulic servo-actuators: MFSW. (Time)	Mass, stiffness, damping and uncertainty.
Conner and Childs (1993)	BS, Air Turbomachinery	L/D = NA, $D = 129.4$, C = NA.	$\omega = 5000 - 16000$, $P = 7.9 - 18.3$.	Disp. transducers,, load cells. Hydraulic shakers: SSW. (Freq.)	Stiffness and damping. (UNR)
Kim and Lee (1994)	ASIS, PAS and HDS, Water, HPOTP.	$L/D = 0.491$, $D = 101.6$, $C = 0.2$, $h = 0.102$	$\omega = 6000$, $P = 10$.	Disp. transducers (eddy-current), Impact hammer: Impulsive. (Freq.)	Stiffness, damping and uncertainty.

Table 1. A chronological summary of the literature on the experimental estimation of the RDPs of seals.

Reference	Type of seals, working fluids and applications	Seal dimensions (mm, wherever applicable)	Speeds (rpm), Reynolds numbers, pressures and pressure differences (bar)	Transducers, exciters and type of excitations (parameter estimation domain)	Parameters estimated (uncertainty analysis)
Ha and Childs (1994)	HS, Air, HPOTP.	$L/D = 1/6$, $D = 152.4$, $C = 0.41$, $w = 0.79$, $h = 2.29$	$\omega = 16000$, $P = 18.3$.	Disp. transducers, accelerometers and quartz load cells. Hydraulic shaker: Sinusoidal. (Freq.)	Stiffness and damping. (UNR)
Brown and Ismail (1994)	LPAS, Water, Centrifugal pumps.	L/D = NA, $D = 100$, $C = 0.25$	$\omega = 3000$, $R_a = 5000$, $R_w = 12120$, $P = 15.6$.	Disp. transducers, accelerometers and load cells. Hydraulic actuator: MFSW. (Time)	Stiffness and damping. (UNR)
Alexander et al. (1995)	PAS, Air, Turbomachinery.	$L/D = 0.334$, $D = 152$, $C = 0.41$, $\alpha = 0 - 0.5$.	$\omega = 16000$, $P = 14.8$.	Disp. transducers, accelerometers and quartz load cells. Hydraulic shaker: PRW. (Freq.)	Stiffness, damping and uncertainty.
Ismail and Brown (1996)	LPAS, Water, Centrifugal pumps.	$L/D = 1$, $D = 100$, $C = 0.25$.	$\omega = 3000$, $P = 15$.	Disp. transducers, accelerometers and load cells. Hydraulic actuator: MFSW. (Time)	Stiffness and damping. (UNR)
Brown et al. (1996)	PAS and JB, Water, Turbomachinery.	$L/D = 1$, $D = 100$, $C = 0.25$.	$\omega = 3000$, $R_a = 5000$, $R_w = 12075$, $P = 15$.	Disp. transducers, accelerometers and load cells. Hydraulic actuator: MFSW. (Time)	Stiffness and damping. (UNR)
Childs and Gansle (1996)	HGAS and HS, Air, Turbomachinery.	$L/D = 0.333$, $D = 152.4$, $C = 0.229$ and 0.305, $\alpha = 0, 15, 30$.	$\omega = 5000 - 16000$, $P = 17$.	Disp. transducers, accelerometers and quartz load cells. Hydraulic shaker: Sinusoidal. (Freq.)	Stiffness, damping and uncertainty.
Vance and Li (1996)	TAMSeal and LS (TOS), Air, Turbomachinery.	L/D = NA, $D = 101.6$, $C = 0.102$ and 0.203	$\omega = 6000$, $P = 4.4$.	Disp. transducers. Unbalance: Sinusoidal. (Freq.)	Stiffness and damping. (UNR)
Marquette et al. (1997)	PAS, Water, Pumps.	$L/D = 0.45$, $D = 77.62$, $C = 0.11$, $\alpha = 0 - 0.5$	$\omega = 10200 - 24600$, $P = 41.4 - 68.9$.	Disp. transducers, accelerometers and load cells. Hydraulic shaker: PRW. (Freq.)	Stiffness and damping. (UNR)
Kaneko et al. (1998)	PASP, Water, Centrifugal pumps.	$L/D = 0.98$, $D = 71.505$, $C = 0.063$ and 0.065	$\omega = 600 - 3000$, $R_a = 125 - 580$, $R_w = 0 - 700$, $P = 29.4$ to 92.5.	Disp. transducers (eddy-current), pressure transducers (strain-gage) and piezoelectric load cells. Eccentric sleeves. (Freq.)	Mass, stiffness, damping and uncertainty.
Ismail and Brown (1998)	LPAS , Water, Centrifugal pumps.	$L/D = 1$, $D = 100$, $C = 0.25$	$\omega = 720 - 3000$, $R_a = 6900 - 12100$, $R_w = 1200 - 6000$, $P = 17$.	Disp. transducers, accelerometers and load cells. Hydraulic actuator: MFSW. (Time)	Mass, stiffness and damping. (UNR)
Childs and Fayolle (1999)	HDS, Water, HPFTP.	$L/D = 0.456$, $D = 76.5$, $C = 0.1$ and 0.12	$\omega = 24600$, $P = 68$.	Disp. transducers, accelerometers and load cells. Hydraulic shaker: PRW. (Freq.)	Mass, stiffness, damping and uncertainty.
Darden et al. (1999)	PAS, Water, SSME	$L/D = 0.5$, $D = 92.51$, $C = 0.533$	$\omega = 20000$, $R = 90000$, $P = 138$, $\Delta P = 93.1$	Disp. transducers (Inductive), accelerometers and piezoelectric load cells. Electrodynamic shaker: Band-limited random excitation (Freq.)	Stiffness, damping and uncertainty.

Table 1. A chronological summary of the literature on the experimental estimation of the RDPs of seals.

Reference	Type of seals, working fluids and applications	Seal dimensions (mm, wherever applicable)	Speeds (rpm), Reynolds numbers, pressures and pressure differences (bar)	Transducers, exciters and type of excitations (parameter estimation domain)	Parameters estimated (uncertainty analysis)
Li et al. (1999b)	MPGDS, Air, Turbomachinery.	L/D = 0.275, D = 127, C = 0.127 – 0.254	ω = 0 – 3000, P = 1.01 – 2.03.	Disp. transducers (eddy-current), pressure sensors (strain-gage) and accelerometer. Impact hammer: Impulsive. (Freq.)	Stiffness and damping. (UNR)
Soto and Childs (1999)	HS and LS, Air, Compressor.	L/D = 0.5, D = 129.79, C = 0.22.	ω = 4680 – 16500, P = 4 to 13.7.	Disp. transducers (eddy-current), accelerometers and quartz load cells. Hydraulic shaker: Sinusoidal. (Freq.)	Stiffness and damping. (UNR)
Ransom et al. (1999)	FPGDS and TBLS, Air, Turbomachinery.	L/D = 0.32, D = 127, C = 0.127 – 0.254.	ω = 3000, P = 1 to 3.	Disp. transducers (eddy-current), pressure sensors (strain-gage) and accelerometer. Impact gun: Impulsive. (Freq.)	Stiffness and damping. (UNR)
Li et al. (2000)	MBPGDS, Air, Turbomachinery.	L/D = 0.25, D = 127, C = 0.127 (inlet) and 0.254 (exit),	ω = 0 – 6000, P = 1.52 to 2.53.	Disp. transducers (eddy-current), pressure sensors (strain-gage) and accelerometer. Impact hammer: Impulsive. (Freq.)	Stiffness and damping. (UNR)
Lindsey and Childs (2000)	TPAS, Water, Centrifugal pumps.	L/D = 0.17, D = 76.2, C(inlet) = 0.076, 0.097 and 0.137. C(exit) = 0.137, 0.097 and 0.076.	ω = 10200 – 24600, ΔP = 13.4 to 34.5.	Disp. transducers (eddy-current), accelerometers and load cells. Hydraulic shaker: PRW. (Freq.)	Mass, stiffness, damping and uncertainty.
Laos et al. (2000)	BHS, PDS and BS, Air, Turbomachinery.	L/D = 0.5, D = 101.6, C = 0.102.	ω = 2000, P = 7.1 bar.	Disp. transducers, Electromagnetic shaker: Periodic Chirp. (Freq.)	Damping and uncertainty.
Kwanka (2000)	SLS and LS (TOS), Air, Turbomachinery.	L/D = 0.306, D = 196, C = 0.5.	ω = 15000, ΔP = 3 bar.	Disp. transducers and forces measured by magnetic bearings. Eccentric rotor. (Freq.)	Stiffness and damping. (UNR)
Kwanka (2001)	SR/HS and LR/HS (with or without SB), Air, Turbomachinery.	L/D = NA, D = 180, C = 0.5, w = 0.8, p = 4, h = 3.75.	ω = 15000, ΔP = 3 bar.	Disp. transducers and forces measured by magnetic bearings. Eccentric rotor. (Freq.)	Stiffness, damping and uncertainty.
Wagner (2001)	LS, SLS and HS, Nitrogen gas, Centrifugal compressor.	L/D = NA, D = NA, C = 0.5.	ω = 10025, P = 250.	Disp. transducers and forces measured by magnetic bearings. Eccentric rotor. (Freq.)	Stiffness and damping. (UNR)
Nielsen et al. (2001)	LR/HS with two SB, Air, HPFTP.	L/D = NA, D = 143.2, C = 0.51.	ω = 5000 – 16000, P = 18.3.	Disp. transducers, accelerometers and quartz load cells. Hydraulic shakers: SSW. (Freq.)	Stiffness, damping and uncertainty.
Darden et al. (2001)	PAS and DS, Water, HPFTP.	L/D = 0.5, D = 91.4, C = 0.53, d = 3.7, h = 0.33 and 0.43.	ω = 3978 – 15764, $R_a = 10^5$, ΔP = 92.9 to 153.6.	Disp. transducers (Inductive), accelerometers and piezoelectric load cells. Electrodynamic shakers: Band-limited random excitation. (Freq.)	Stiffness, damping and uncertainty.

Table 1. A chronological summary of the literature on the experimental estimation of the RDPs of seals.

Reference	Type of seals, working fluids and applications	Seal dimensions (mm, wherever applicable)	Speeds (rpm), Reynolds numbers, pressures and pressure differences (bar)	Transducers, exciters and type of excitations (parameter estimation domain)	Parameters estimated (uncertainty analysis)
Holt and Childs (2002)	HSAGS and PAS, Air, Centrifugal compressor.	L/D = 0.75, D = 114.3, C = 0.203, d = 1.59, h = 2.03 and 3.18.	ω = 20200, P = 17.2.	Disp. transducers (eddy-current), accelerometers and load cells. Hydraulic shaker: PRW. (Freq.)	Freq. dependent stiffness and damping and uncertainty.
Dawson et al. (2002)	PAS, Air, Centrifugal compressors.	L/D = 0.75. D = 114.3, C = NA.	ω = 20200, P = 17.2.	Disp. transducers (eddy-current), accelerometers and load cells. Hydraulic shaker: PRW. (Freq.)	Freq. dependent stiffness and damping and uncertainty.
Dawson and Childs (2002)	PAS and HS, Air, Centrifugal compressor.	L/D = 0.75, D = 114.3, C = 0.19, h = 3.10, w = 0.79.	ω = 20200, P = 17.2.	Disp. transducers (eddy-current), accelerometers and load cells. Hydraulic shaker: PRW. (Freq.)	Freq. dependent stiffness and damping and uncertainty.
Weatherwax and Childs (2003)	HS, Air, Centrifugal compressor.	L/D = 0.75, D = 114.74, C = 0.178, w = 0.79, h = 3.10, α = 0 – 0.5.	ω = 20200, P = 70.	Disp. transducers (eddy-current), accelerometers and load cells. Hydraulic shaker: PRW. (Freq.)	Eccentricity dependent stiffness and damping and uncertainty.
Kaneko et al. (2003)	TDSHR, SDSHR and PAS, Water, Pumps.	L/D = 0.84, D = 71.4, C = 0.176 and 0.168.	ω = 3000, R_a = 0 – 2000, R_w = 2500 – 4800, ΔP = 7.84.	Disp. transducers (eddy-current), pressure transducers (strain-gage) and piezoelectric load cells. Eccentric sleeves. (Freq.)	Stiffness, damping and uncertainty.
Childs and Wade (2004)	HSAGS, Air, HPOTP.	L/D = 0.75, D = 134.7, C = 0.1 – 0.2, d = 3.18, h = 3.30.	ω = 15200, R_a = 10^5, P = 70.	Disp. transducers (eddy-current), accelerometers and load cells. Hydraulic shaker: PRW. (Freq.)	Freq. dependent stiffness and damping and uncertainty.

Abbreviations. Acc., acceleration; ASIS, antiswirl self-injection seals; BHS, brush hybrid seal; BS, brush seal; $CBrF_3$, trifluro-bromomethane; DDS, diamond-grid pattern damper seals; Disp., displacement; FPGDS, four-pocket gas damper seal; Freq., frequency; HDS, hole-pattern damper seal; HGAS, helically grooved annular seals; HGS/SR, helically grooved stator with smooth rotor; HPFTP, high-pressure fuel turbopump; HPOTP, high-pressure oxygen turbopump; HS, honeycomb seals; HSAGS, hole-pattern stator annular gas seals; HS/SR, honeycomb stator with smooth rotor; JB – Journal bearing; LPAS – Long plain annular seals; LR/HS – Labyrinth rotor with honeycomb stator; LS – Labyrinth seals; MBPGDS – Multiple-blade, multiple-pocket gas damper seal; MPGDS, multiple-pocket gas damper seal; MFSW, multifrequency sine wave; NA, not available; PAS, plain annular seals; PASP, plain annular seal with porous material; PDS, pocket damper seals; RDS, round-hole-pattern damper seals; SB, swirl brake; SDS, saw-tooth pattern damper seals; SDSHR, straight damper seals with honeycomb roughness; SLS, stepped labyrinth seal; PRW, pseudo-random waveform; SS, screw seals; SSW, swept sine wave; SSME, space shuttle main engine; TAMSeal, a new type of labyrinth seal developed in Texas A&M University; TBLS, two-bladed labyrinth seal; TDS, triangular pattern damper seals; TDSHR, tapered damper seals with honeycomb roughness; TOR, teeth on rotor; TOS, teeth on stator; TPAS, tapered plain annular seals; UNR, uncertainty not reported.
Symbols. L, seal length; R, seal radius; C, seal clearance; D, seal diameter; h, depth/height of hole or different patterns; d, diameter of the hole pattern; w, width of the triangular (or other) pattern; p, pitch of the teeth (in labyrinth); R, Reynolds number; R_a, axial Reynolds number; R_w, circumferential Reynolds number; ΔP, pressure (maximum or inlet); DP, pressure difference; α , helix angle; ε, eccentricity ratio; ω, rotor spin speed.

place between two surfaces having relative movement, i.e. rotary, reciprocating, and oscillating. The main focus of this paper is on rotary seals. These have a wide variety of applications in high-speed, high-pressure, and cryogenic temperature conditions in the aviation and space industries, such as in turbine stages, turbopumps, compressors, gear boxes, etc. Rotary seals can be subdivided into two main categories: clearance seals and contact seals. Clearance seals are circumferential non-contacting seals (Figure 2(a)). In contact seals, the contact is formed by positive pressure, while clearance seals operate with positive clearance (no rubbing contact). The most commonly used materials for dynamic seals (especially for rotary seals) are stainless steel, bronze, aluminum, nickel-based alloys, polytetrafluroethane, etc.

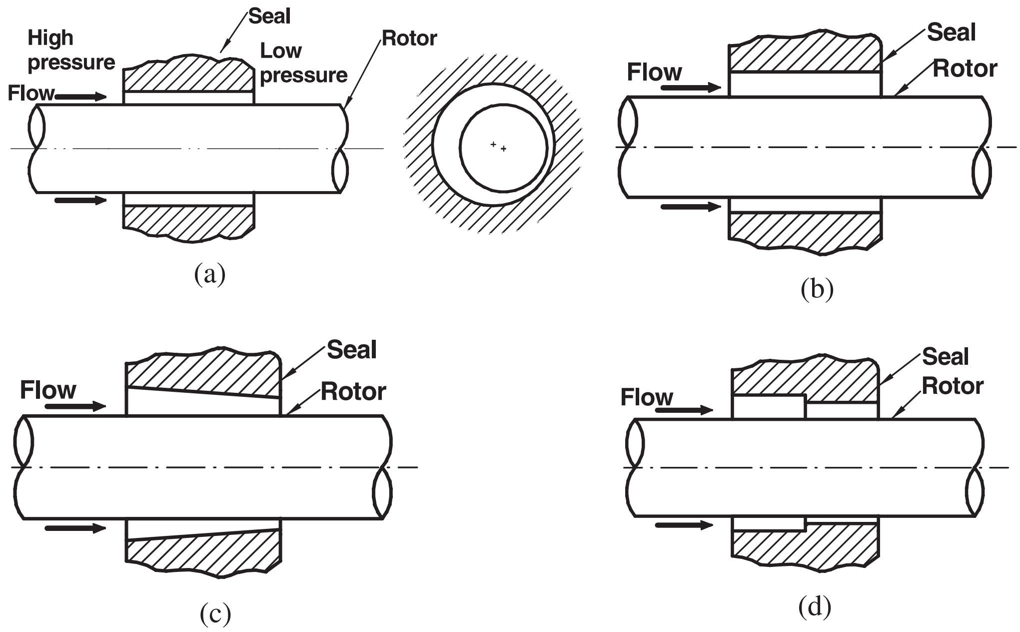

Figure 2. (a) Rotor-seal assembly. (b) Straight annular seal. (c) Tapered annular seal (converging). (d) Stepped annular seal.

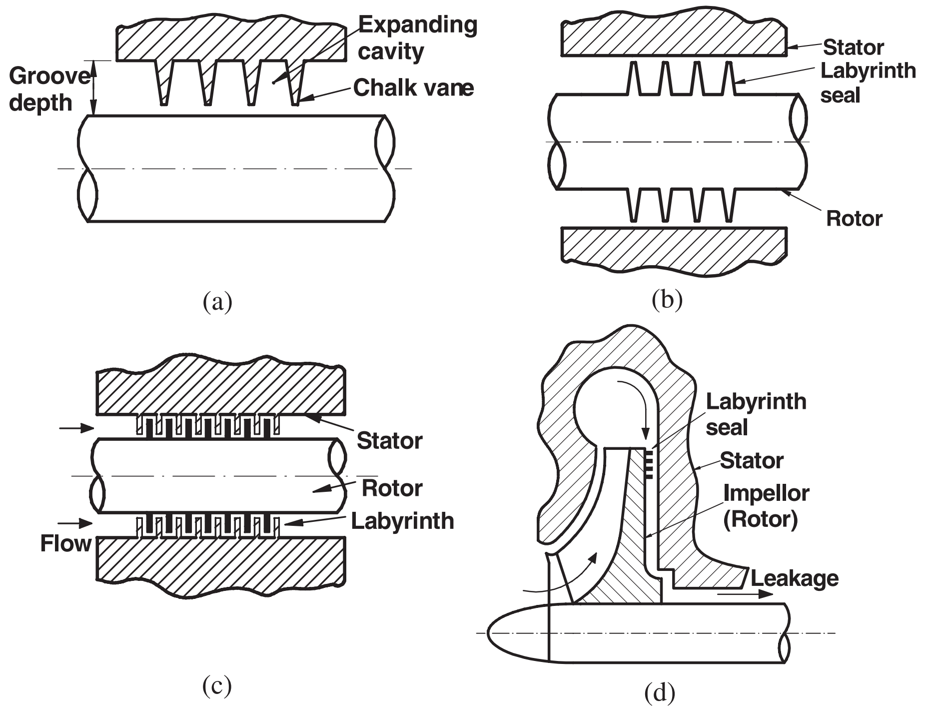

Figure 3. (a) Labyrinth seal (teeth-on-stator). (b) Labyrinth seal (teeth-on-rotor). (c) Labyrinth seal (teeth-on-stator and teeth-on-rotor) axial flow type. (d) Labyrinth seal radial flow type.

Figure 2(a) shows a typical rotary seal with the clearance exaggerated. Rotary seals based on geometry can be classified as follows.

(i) Ungrooved plain seals (or smooth annular seals): (a) straight (Figure 2(b)); (b) tapered (Figure 2(c)) and (c) stepped (Figure 2(d)). In geometry they are similar to journal bearings but the clearance/radius ratio is as low as two times and as high as ten times (or more) larger to avoid rotor/stator contact.

(ii) Grooved/roughened surface seals: (a) porous surface seals; (b) labyrinth seals (Figures 3(a)–(d)); (c) helically

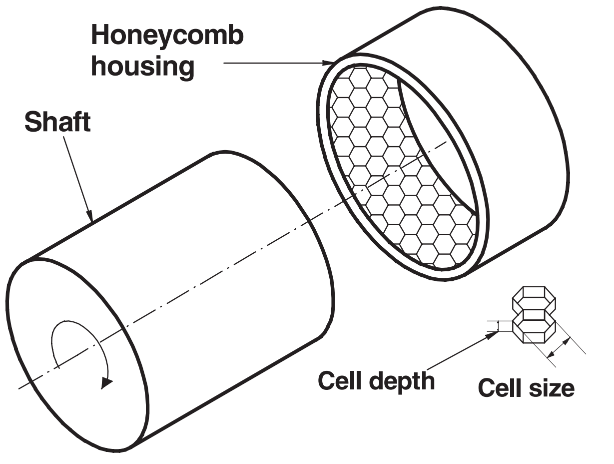

Figure 4. Honeycomb seal.

grooved/screw seals; (d) circular hole or triangular patterns seals; (e) honeycomb pattern seals (Figure 4). These seals are used in centrifugal and axial compressors and pumps and in turbines. Different internal surface patterns of seals are shown in Figure 5.

(iii) Contact seals: (a) brush seals (Figure 6(a)); (b) face seals; (c) lip seals (Figure 6(b)). Because of rubbing, these seals are used commonly in low-speed pumps, or where the working fluid can act as a coolant. Contact seals provide much lower leakage rates than either of the non-contact seals (Adams, 1987); however, the latter can operate at very high speed and pressure conditions.

(iv) Floating-ring oil seals. The ring whirls or vibrates with the rotor in the lubricating oil, but does not spin. These are used in high-pressure multistage centrifugal compressors.

1.2. Theoretical and Computational Analysis

In this subsection, we have compiled the theoretical and computational analyses performed by various researchers. Lomakin (1958) was the first to propose a theoretical model of a plain seal, which predicted that the axial pressure drop across the seal caused a radial stiffness, independent of shaft rotation. The Lomakin radial direct stiffness (k_d) is given by

$$k_d = 4.7R\left(\frac{\Delta P}{\lambda}\right)\left(\frac{\lambda L/C}{1.5 + 2\lambda L/C}\right)^2 \qquad (1)$$

$$\text{with} \quad \lambda = 0.079/R_e^{0.25}$$

where ΔP is the pressure drop, and R, L, and C are the radius, axial length, and radial clearance of the seal, respectively. If the direct stiffness were the only effect of the plain seal, then its effect on critical speeds would be easily and accurately predictable. Black (1969, 1971) provided the major initial impetus for the extensive research and the state-of-the-art design information developed on this topic over the last 35

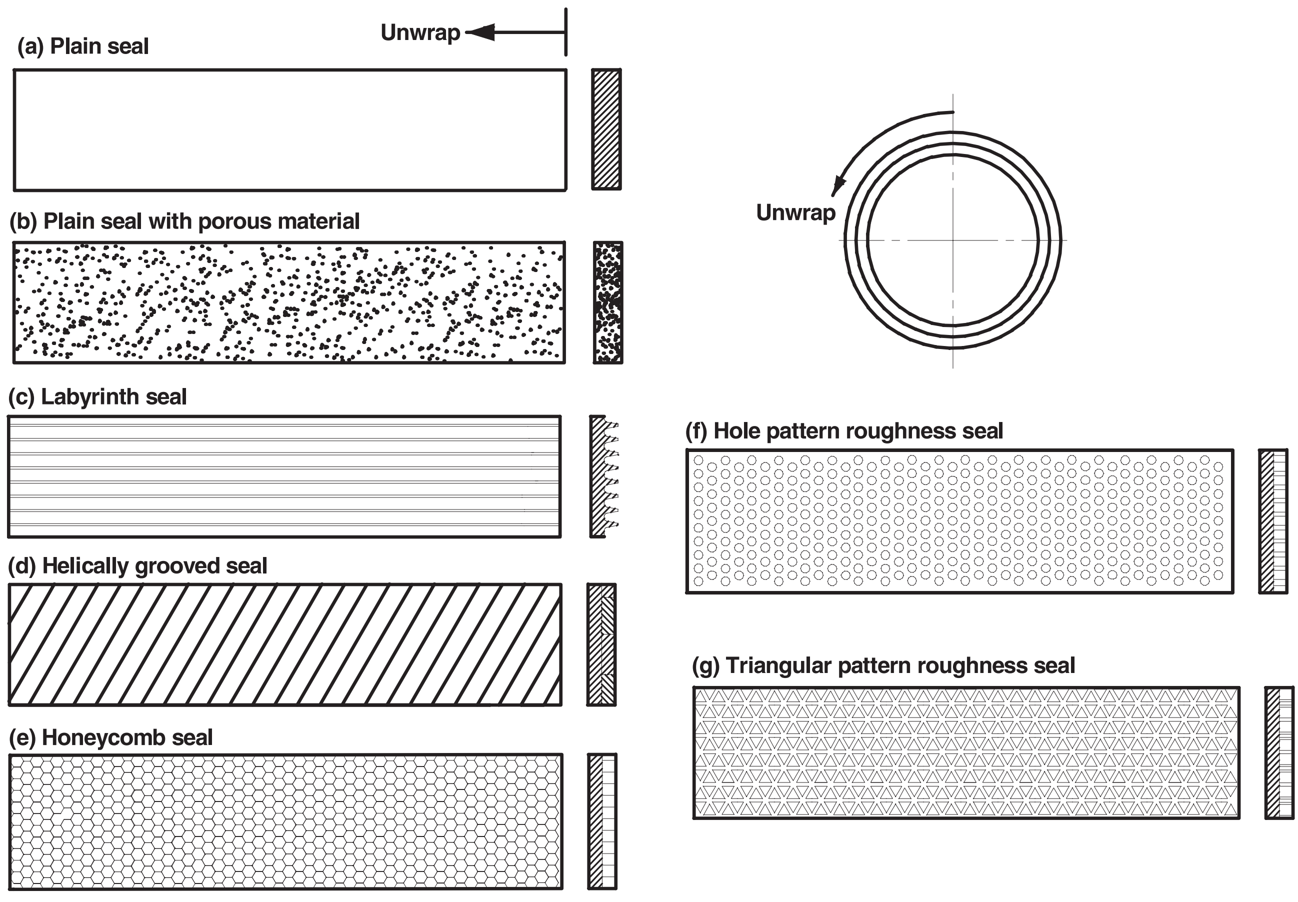

Figure 5. Different internal surface patterns on seals.

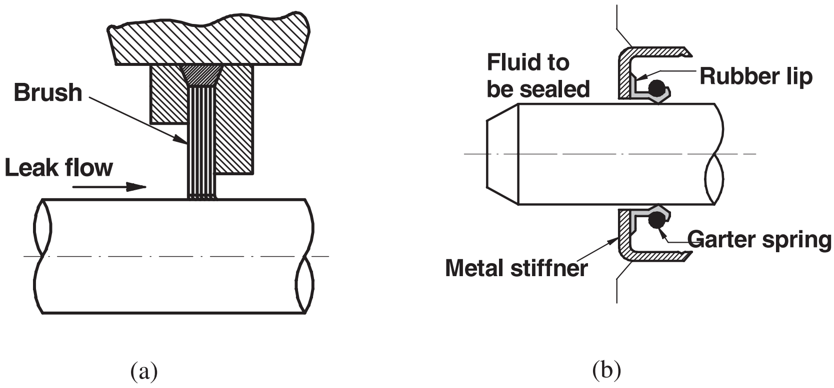

Figure 6. (a) Brush seal. (b) Lip seal.

years. Black developed the classical theory for turbulent annular seals, considering the axial fluid flow caused by a pressure drop along the seal, the rotational fluid flow as a consequence of the shaft rotation, and a relative motion of the seal between the rotor and housing. Black (1969, 1971) and Childs (1983a, 1983b) formulated and extended Lomakin's theory in terms applicable to the rotor dynamic analysis of centrifugal pumps. Black, Childs and others have shown, however, that k_d increases with shaft speed (at constant ΔP) and that the seal also produces cross-coupled stiffness (k_c), direct and cross-coupled damping (c_d and c_c), and direct inertia coefficients. Moreover, the pressure drop will vary with the speed in most turbomachinery and the rotor dynamic effects are quite complex. Kirk and Miller (1977) studied the influence that high-pressure oil seals have on turbocompressor stability, introducing some design guidelines to avoid the appearance of subsynchronous vibrations. Allaire et al. (1978) carried out a perturbation analysis for eccentric plain seals with high axial flow rates and calculated the load capacity, stiffness, and damping of the seals for a wide range of axial Reynolds number. Also, the design parameters for a three-stepped plain seal were calculated for the space shuttle main engine hydrogen turbopump. Falco et al. (1984) used a mathematical model, which is based on the Reynolds equation using the turbulence factors derived from the bulk-flow theory (Hirs, 1973) for predicting the dynamic behavior of plain liquid seals. The bulk-flow model uses Hirs' turbulent-lubrication model using three variations of the Blasius (1913) pipe-friction model: (i) a basic model where the Reynolds number is a linear function of the local clearance; (ii) a model where the coefficient is a function of the local clearance; (iii) a model where both the coefficient and exponent are functions of the local clearance. Wyssmann et al. (1984) presented an analysis for calculation of stiffness and damping coefficients of the fluid–rotor interaction in centrifugal compressor labyrinth seals based on turbulent flow calculations. Kirk (1985) developed a compressor design taking into account the interaction of labyrinth seals with the rotor, and addressed the importance of the design of labyrinth seal clearances to enhance stability. Kirk (1986) reviewed the analysis of the loading and hydrodynamic forces applied to typical oil-seal design studies. Limitations of analysis capabilities and recommendations for the future analysis and testing required to fully understand the dynamic operation on oil-seal rings and their influence on the dynamic stability of high-speed, high-pressure, flexible shaft turbocompressors were discussed. Childs and Kim (1985) developed a combined analytical–computational method to calculate the leakage, transient pressure field and RDPs for high-pressure annular damper seals using the Hirs (1973) turbulent lubrication equations and perturbation techniques. Based on a similar method, Childs and Dressman (1985) analyzed tapered high-pressure annular seals. A short-bearing approximation was used to derive an analytical expression for the first-order (dynamic) pressure gradient. This expression was integrated numerically to define RDPs for the seal. Dietzen and Nordmann (1987) solved the Navier–Stokes equations using the finite-difference method for modeling the turbulent flow in a seal. Kirk (1988) analyzed floating ring liquid seals and evaluated the seal ring dynamic transient response including stick–slip on the axial sealing face and the ring spin torque interaction with the antirotation element. The static and dynamic characteristics of annular plain seals were investigated theoretically in the turbulent flow regime by Simon and Frêne (1989). Scharrer and Nelson analyzed, for both incompressible (Scharrer and Nelson, 1991a) and compressible flows (Scharrer and Nelson, 1991b), partially tapered annular seals. They used Hirs' turbulent lubrication equations and perturbation techniques in their analysis. Childs (1993) gave an excellent compilation of work on plain annular seals along with other kinds of seals. Krämer (1993) and Rao (2000) described a simple, however, a crude and an iterative procedure to calculate plain seal RDPs (i.e. k_d, c_d, k_c, and c_c) and they gave a comprehensive list of publications on seal dynamics. Reedy and Kirk (1992) presented the heat balance calculations required for determination of the pressure and temperature distributions and enforcing consistent leakage flows for the multiland and/or multiring seals, which can be used for calculation of RDPs for each ring of the seal assembly. Baheti and Kirk described a finite-element solution of the nonlinear and coupled hydrodynamic and thermal equations for pressure and temperature profiles in a floating oil ring seal including misalignment and axial taper (Baheti and Kirk, 1994) and the influence of circumferential grooves (Baheti and Kirk, 1995). Baheti et al. (1996) presented the analytical results for the axially grooved floating oil ring seals on the leak flow and stability of a centrifugal gas compressor for both low- and high-pressure sealing conditions. Results have shown that the added grooves enhance the stable operation of the rotor system for low-pressure fixed seal conditions and reduce the system stability at lower eccentricities for low-pressure floating seal conditions. In high-pressure conditions, added grooves enhance the stability of the system for both fixed and floating seal conditions. Kirk and Baheti (1997) presented guidelines for the design of liquid rings of straight, tapered, and circumferentially grooved geometries, which could be useful for the application of high-performance compressor liquid seal designs. Numerical results including the RDPs were also presented for different geometries. Baheti and Kirk (1999) presented results comparing the seal leakage, seal oil outlet temperatures, stiffness and damping coefficients, and damped natural frequencies from the thermo hydrodynamic analyses with and without the influence of the mechanical deformation of the bushing seal ring using the finite-element method. Oike et al. (1999) carried out a flow visualization study on the two-phase flow in floating-ring seals for cryogenic fluid to identify the two-phase flow area inside the sealing clearance induced by the viscous frictional heating and the pressure drop; they also investigated the effect of the two-phase flow area on the leakage.

Alford (1964) reported an accident due to labyrinth seals in which the mechanism of the occurrence of unstable vibration was explained by considering energy input due to the phase difference between the rotor deflection and the fluid reaction force (Alford, 1965). However, vortex and viscosity are not considered in his analysis. The high axial fluid velocity through the seal and the relatively large clearance produce a highly turbulent flow condition in the seal, which violates the Reynolds assumption of laminar flow, and hence the Reynolds theory is inapplicable, even if fluid inertia effects are added. In an analytical study, Murphy and Vance (1980) extended Alford's analysis to multibladed seals, considering choked flow to be possible only at the last (exit) blade. Iwatsubo et al. (1982) published the analytical basis of a computer program to predict seal RDPs; however, conformation with the experimental results was not so good. Scharrer (1988) used a perturbation analysis to linearize the governing equations of honeycomb stator seals. The model provided accurate predictions of direct damping (c_d) for large clearance seals; however, the model predictions and test results diverged with the increasing running speed. Elrod et al. (1989) developed an entrance region shear stress model for duct flow. A bulk-flow gas seal analysis using this model instead of an entrance-loss coefficient predicted the leakage and stability characteristics of honeycomb-stator/smooth-rotor. However, Childs et al. (1989) observed that the main reason for the disagreement between the theory and experiments was the inadequacy of the fluid friction model in the analysis. The turbulence model, which uses the nonlinear analysis developed by Elrod and Ng (1967), was improved for Reynolds numbers higher than 10^5 to include cryogenic application. In addition, velocity boundary conditions were modified. A comparison of predictions based on this analysis with the Childs (1983a, 1983b) incompressible flow solution and the Nelson and Nguyen (1987) compressible flow solution were in agreement.

Elrod et al. (1990) developed the entrance and exit region friction factor models using wall shear stress results from stationary-rotor flow tests of annular gas seals, and used these friction factor models in a bulk-flow analysis to predict the leakage and RDPs. Kirk (1990) presented a method for calculating the inlet swirl at the entrance of the labyrinth seal, and the solution included the friction factors taking into account the mass flow rate and the calculation of radial pressure gradients by a free vortex solution. Wilkes et al. (1993) presented an analysis procedure which determined the RDPs for circumferentially grooved annular seals with turbulent incompressible flow using Hirs' turbulent lubrication theory as the basis for the governing equations and theory for a turbulent shear layer as the basis for friction factors in the groove. Padavala et al. (1993) developed a theory to predict RDPs based on the bulk flow model using the Hirs' friction factor model. An empirical friction-factor model for honeycomb surfaces based on flat plate test results was developed by Ha and Childs (1994) as a function of Mach number and dimensionless pressure and honeycomb geometry variables (the radial clearance and the cell width). A rotor dynamic analysis for centered, turbulent-annular-honeycomb-stator seals was developed incorporating an empirical friction-factor model for honeycomb stator surfaces. Results of the analysis in predicting RDPs and leakage characteristics were compared to (a) Moody's friction-factor model analysis and (b) experimental data (Childs and Kleynhans, 1992) for short seals. Comparisons showed that their honeycomb friction-factor model improved the predictions of the leakage and RDPs compared to Moody's friction-factor model, especially, for the direct and cross-coupled stiffness.

San Andrés (1991) developed a computer code that solved two-dimensional, bulk-flow, incompressible, Navier–Stokes equations to predict the static and rotor dynamic characteristics of bearings and seals, in centered and eccentric positions. A perturbation analysis was performed. Kleynhans and Childs (1997) presented a two-control-volume model for honeycomb-stator/smooth-rotor seals with a conventional control volume used for the through-flow and a "capacitance accumulator" model for the honeycomb cells. Li et al. (1999a) used a one-control volume, turbulent bulk-flow model for the prediction of the seal leakage and RDPs of multiple-pocket damper seals. Based on Kleynhans and Childs (1997) model, Dawson and Childs (2002) determined seal leakage flow-rate and direct and cross-coupled impedances for a constant temperature, two-control-volume annular gas seal. D'Souza and Childs (2002) used a two-control-volume bulk-flow model to predict RDPs for an annular, honeycomb-stator/smooth-rotor gas seal. Yücel (2003) calculated the leakage and RDPs of stepped labyrinth gas seals using the continuity and circumferential momentum equations for the compressible flow. Results were compared with the experimental results of Kwanka (2000). Moore (2003) presented a three-dimensional computational fluid dynamics (CFD) to model the labyrinth seal flow path by solving the Reynolds averaged Navier–Stokes equations. To calculate rotor dynamic forces, a full three-dimensional, eccentric model was solved. In comparison to experimental leakage and RDPs (Pelletti and Childs, 1991) good agreement was found over bulk-flow approaches. Arghir and Frêne (2004) introduced a numerical solution of the three control-volume, bulk-flow model suitable for analyzing eccentric circumferentially grooved liquid annular seals. Forces arising from perturbations were obtained by integrating the first-order pressure field and expressed via RDPs. The comparison with experimental results (Marquette and Childs, 1997) was found to be good. Table 2 summarizes a comparison of different theoretical analysis proposed

Table 2. Comparison of the theoretical analysis with experimental investigations.

Experimental investigations (reference)	Theoretical analysis (reference)	Comparison with experimental investigations					
		Direct stiffness	Cross-coupled stiffness	Direct damping	Cross-coupled damping	Leakage	General remarks
Falco et al. (1984)	Model based on Reynolds equation with turbulent factor	Poor (low)	High	Good	Poor (low)	Good	Good agreement
Nordmann and Massmann (1984)	Black (1969) analysis	High (40% error) for speed variation	90% of difference for speed variation	___	___	___	Good agreement for axial velocity variation in mass, stiffness and damping coefficients
Childs and Kim (1985)	Model based on Hirs (1973) lubrication equations	Poor (low)	___	___	___	___	Net damping and added mass coefficients were overpredicted
Elrod et al. (1989)	Elrod et al. (1990)	Poor	Good	Good	___	Good	
Hawkins et al. (1989)	Scharrer (1988) two-control volume model		Predicts within 25%	Underpredicts at low speeds	___	___	Better results for larger clearances
Simon and Frêne (1989)	Elrod (1967), Ng and Pan (1965) turbulent model with Reynolds equation	Good	Good	Better for long seals than short seals	Poor	Good	Experimental results are from Kanki and Kawakami (1984)
Childs et al. (1990a)	Elrod et al. (1990)	Poor (worst at higher pressure ratios)	Low	___	High	___	
Childs et al. (1990b)	Kim and Childs (1987)	Good	Poor	___	___	Good	Predictions were wrong for effective damping coefficients
Kanemori and Iwatsubo (1992)	Childs (1982)	Good	Good	Good	Good	___	Added mass and moment coefficients were also predicted
Ha and Childs (1992)	Moody's friction factor model	Overpredicted	Good	Overpredicted	Overpredicted	___	
Ha and Childs (1994)	Friction-factor model based on flat plate results (Nelson and Nguyen, 1987)	Overpredicted but improved as compared with Moody's model	Better	Overpredicted	Overpredicted but improved as compared with Moody's model	___	This model was compared with the Moody's friction factor model
Alexander et al. (1995)	Yang (1993)	Overpredicted	Good	Underpredicted at low pre-swirl values	Good	___	
Marquette et al. (1997)	San Andrés (1991)	Slightly underpredicted	Good	Overpredicted except at high eccentricities	Good	Accurate	Direct inertia agrees well with predictions
Darden et al. (1999)	Padavala et al. (1993)	Excellent	Good	Good	Good	___	Overall good agreement

Table 2. Comparison of the theoretical analysis with experimental investigations.

Experimental investigations (reference)	Theoretical analysis (reference)	Comparison with experimental investigations					
		Direct stiffness	Cross-coupled stiffness	Direct damping	Cross-coupled damping	Leakage	General remarks
Li et al. (1999b)	One control volume and bulk flow model (Li et al., 1999a).	Underpredicted	Satisfactory	Overpredicted	___	Slightly over-predicted	
Kwanka (2000)	Yücel (2003)	Poor (low)	Good	Poor (Low)	Poor (Low)	Low	
Dawson and Childs (2002)	Kleynhans and Childs (1997)	Underpredicted	Deviated by 31%	Underpredicted	Deviated by 22%	Good	RDP predictions were very good
Moore (2003)	Pelletti and Childs (1991)	Good	Good	Underpredicted	___	___	
Arghir and Frêne (2004)	Marquette and Childs (1997)	Low	Low	Very low	Low	Good	

with the experimental results. Guo and Kirk (2005) used ANSYS–TASCFlow, a commercial CFD program, to simulate the leak path and labyrinth seal of two different covered centrifugal compressor eye seals. For each case, three-dimensional models with eccentric rotors were solved to obtain the leakage flow, velocity vector, chamber pressure, average chamber swirl, and the rotor dynamic force components. Nakamura and Iwatsubo (2005) calculated distributions of the circumferential velocity and the pressure in the pre-swirl groove (inlet of the seal) and the effect of the velocity and pressure distributions on the flow-induced dynamic force. The results were compared with conventional type seals in order to know how much the instability force could be reduced. Also, the results were compared with the results calculated by assuming the circumferential velocity of the pre-swirl groove as half the speed of the injection velocity. Iwatsubo et al. (2005) presented static and dynamic design data to decide the seal configuration for obtaining the high efficiency and the stable rotor system; that is, when constraints and conditions of the seal are given, the optimum seal configuration (fin heights, widths, clearances, number of fins, and so on) can be decided.

1.3. Fluid-Film Dynamic Force Equations

A model of a typical annual (or clearance) seal is shown in Figure 2(a). The geometrical shape of a clearance seal is similar to that of a hydrodynamic bearing; however, they are different in the following aspects. To avoid contact between a rotor and a stator, the ratio of the clearance to the shaft radius in seals is made a few times (two to ten times) larger than that of hydrodynamic bearings. The flow in seals is turbulent and in hydrodynamic bearings it is laminar. Therefore, unlike a hydrodynamic bearing, we cannot use the Reynolds equation for analysis of seals. When a rotor vibrates, a reaction force of the fluid in the seal acts on the rotor. In the case of a small vibration around the equilibrium position, the fluid force can be linearized on the assumption that deflections Δx and Δy are small. The general governing equations of fluid-film forces on seals, which have small oscillations relative to the rotor, are given by the following linearized force–displacement model (Childs et al., 1986)

$$-\begin{Bmatrix} f_x \\ f_y \end{Bmatrix} = \begin{bmatrix} k_{xx} & k_{xy} \\ k_{yx} & k_{yy} \end{bmatrix}\begin{Bmatrix} \Delta x \\ \Delta y \end{Bmatrix} + \begin{bmatrix} c_{xx} & c_{xy} \\ c_{yx} & c_{yy} \end{bmatrix}\begin{Bmatrix} \Delta \dot{x} \\ \Delta \dot{y} \end{Bmatrix} + \begin{bmatrix} m_{xx} & m_{xy} \\ m_{yx} & m_{yy} \end{bmatrix}\begin{Bmatrix} \Delta \ddot{x} \\ \Delta \ddot{y} \end{Bmatrix} \quad (2)$$

where f_x and f_y are the fluid-film reaction forces on seals in the x and y directions. k, c, and m represent the stiffness, damping, and added-mass coefficients, respectively, the subscripts xx and yy represent the direct terms, and the subscripts xy and yx represent the cross-coupled terms. These coefficients vary depending on the equilibrium position of the rotor (i.e. magnitude of the eccentricity), rotational speed, pressure drop, temperature conditions, etc. The off-diagonal coefficients in equation (2) arise due to fluid rotation within the seal, and unstable vibrations may appear due to these coefficients. Equation (2) is applicable to liquid annular seals. However, for the gas annular seals, the added-mass terms are negligible. For small motion about a centered position (or with very small eccentricity) the cross-coupled terms are equal and opposite (e.g. $k_{xy} = -k_{yx} = k_c$ and $c_{xy} = -c_{yx} = c_c$) and the diagonal terms are same (e.g. $k_{xx} = k_{yy} = k_d$ and $c_{xx} = c_{yy} = c_d$; Childs et al., 1986). Considering these relationships and neglecting the cross-coupled added-mass terms, equation (2) takes the following form:

$$-\begin{Bmatrix} f_x \\ f_y \end{Bmatrix} = \begin{bmatrix} k_d & k_c \\ -k_c & k_d \end{bmatrix}\begin{Bmatrix} \Delta x \\ \Delta y \end{Bmatrix} + \begin{bmatrix} c_d & c_c \\ -c_c & c_d \end{bmatrix}\begin{Bmatrix} \Delta \dot{x} \\ \Delta \dot{y} \end{Bmatrix} + \begin{bmatrix} m_d & 0 \\ 0 & m_d \end{bmatrix}\begin{Bmatrix} \Delta \ddot{x} \\ \Delta \ddot{y} \end{Bmatrix}. \quad (3)$$

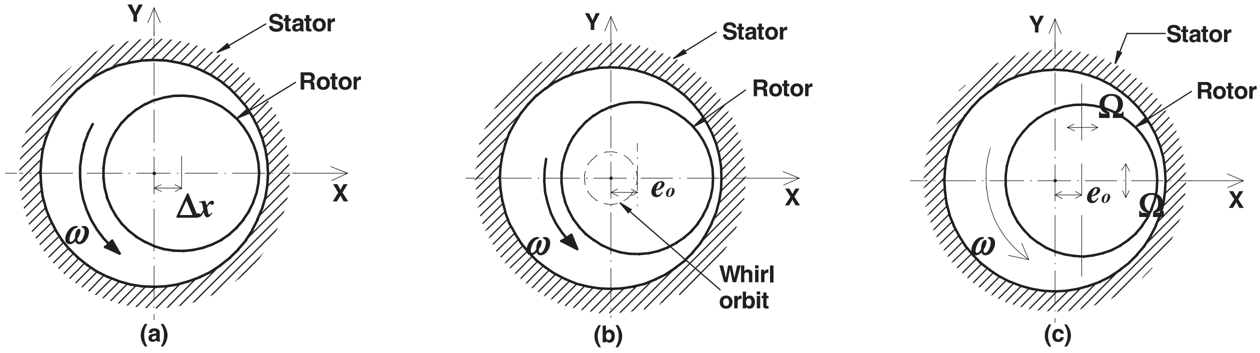

Figure 7. (a) Rotor with static displacement; (b) eccentric rotor; (c) external shaker excitation.

Here, subscripts d and c represent direct and cross-coupled, respectively. The RDPs largely affect the performance of the turbomachinery as they lead to serious synchronous and subsynchronous vibration problems. The whirl frequency ratio, $f = k_c/(c_d\omega)$, is a useful non-dimensional parameter for comparing the stability properties of seals. For circular synchronous orbits, it provides a ratio between the destabilizing force component due to k_c and the stabilizing force component due to c_d. In the experimental estimation of the RDPs of seals, these coefficients (of equations 2 and 3) are determined with the help of measured vibrations data from a seal test rig.

1.4. Experimental Estimation Procedures

In this subsection, various seal test approaches used for the estimation of RDPs for governing equations of the form of equation (3) of seals are reviewed with a schematic representation. In the method used by Benkert and Wachter (1980), the seal rotor (Figure 7(a)) is statically displaced relative to its stator, the circumferential pressure distribution is measured and integrated, and the resultant reaction force is calculated. This method does not yield any damping values since only static load is applied. Referring to equation (3), the static rotor displacement Δx in the X direction yields (while keeping $\Delta y = 0$)

$$k_d = f_x/\Delta x \quad \text{and} \quad k_c = f_y/\Delta x. \tag{4}$$

Figure 7(b) describes the rotor motion relative to the stator that represents two different types of rotor excitation arrangement, i.e. eccentric rotor (Childs and Garcia, 1987) and eccentric sleeves (Kanemori and Iwatsubo, 1992). The varying clearances modulated the local flows in and out of the seal and circumferentially in the seal annulus, and thereby caused the static pressure in the seal annulus to vary circumferentially and periodically. At each instant, the varying component of the static pressure has an essentially sinusoidal distribution around the circumference, and this pressure pattern rotates in synchronism with rotor whirl. The circumferential pressure distribution was measured and integrated to obtain the resultant reaction forces acting on the rotor. The centered circular orbit is defined by $x = e_o\cos(\Omega t)$ and $y = e_o\sin(\Omega t)$, where Ω is the frequency of excitation, e_o is the whirl radius, and t is the instant time. Hence, an equation of the form of equation (3) yields the following radial and circumferential coefficient (subscripts r and θ, respectively) definitions

$$F_r/e_o = -k_d - c_c\omega + m_d\omega^2 \quad \text{and} \quad F_\theta/e_o = k_c - c_d\omega \tag{5}$$

where k, c, and m represent the stiffness, damping, and added-mass coefficients, and subscripts d and c represent the direct and cross-coupled terms, respectively. The test rig is used to measure F_r/e_o and F_θ/e_o versus Reynolds number and rotor rotational frequency, ω. Iwatsubo et al. (1990) and Kaneko et al. (1998) assumed seal RDPs independent of ω and used the measured F_r/e_o and F_θ/e_o with respect to ω, for curve-fitting to obtain RDPs, i.e. k_d, k_c, c_c, c_d, and m_d. Kanemori and Iwatsubo (1992) used a similar procedure, except that the dynamic moment coefficients were also identified. The form of the moments due to the fluid-film was similar to that of equation (3) with corresponding moment coefficients (e.g. $k_{\theta\theta}$, $k_{x\theta}$ etc., where θ is the transverse angular displacement). The rotor was independently driven by two motors to realize the spinning and whirling motion.

For the case when seal RDPs depend upon ω, equation (3) can be approximated with the assumption that k_c and c_c vary linearly with ω, as (Childs, 1993)

$$F_r/e_o = -k_{ef} + m_{ef}\omega^2 \quad \text{and} \quad F_\theta/e_o = -c_{ef}\omega. \tag{6}$$

When measurements are obtained for a fixed axial Reynolds number over a range of ω, the above equations can be used to curve-fit to obtain effective RDPs, i.e. k_{ef}, c_{ef}, and m_{ef}. This approach eliminates RDP dependency on ω.

Wright (1978, 1983) proposed a method in which a centered circular whirling orbit (Figure 7(c)) was obtained by an active feedback system. The conceptual approach (Childs et al., 1986), which is used in the estimation of RDPs for small motion about the static eccentricity position, is shown in Figure 7(c), defined by the coordinates (e_o, 0). For this position, the shaker applies the harmonic horizontal motion with an excitation frequency Ω (a calibrated imbalance can also be used with $\omega = \Omega$, where ω is the rotor spin speed or the system (preferably housing) can be excited by an impact of the hammer with a multifrequency excitation). On substituting measured forces and displacement data into equation (2), for a given operating condition, using curve-fitting techniques the RDPs for seals can be obtained. A detailed account of

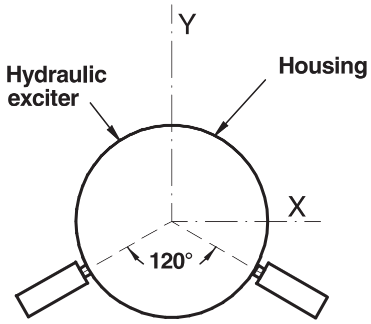

Figure 8. An excitation system configuration.

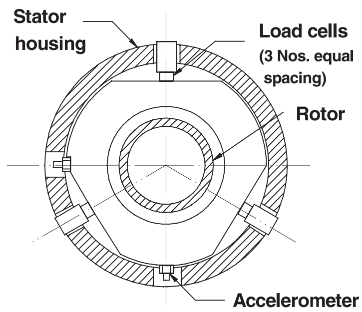

Figure 9. End view of the stator mounting assembly (Childs et al., 1986).

general estimation procedures can be found in Tiwari et al. (2002, 2004).

1.5. Previous Seal Rotor Dynamic Data and Resources

Allaire and Flack (1982) presented a partial review of the literature on lateral impeller forces by considering the case studies for coolant pumps. Flack and Allaire (1984a) critically reviewed the hydraulically generated lateral forces in pumps. The experimental measurement of pressures, static forces and dynamic forces in pumps were also reviewed. Flack and Allaire (1984b) reviewed the static and dynamic characteristics of tilting pad and turbulent hydrostatic journal bearings. Etison (1982, 1985) reviewed the experimental observations and theoretical analyses of face seal dynamics. The more recent textbooks on rotor dynamics include information on rotor dynamic characteristics of rotary seals. Vance (1988), Krämer (1993), Rao (2000), and Adams (2001) provide good introductory treatments of seal dynamics. However, one of the first surveys, and a comprehensive survey, of the literature related to the experimental estimation of RDPs of seals was made by Childs (1993). Until the present, it has been the single most valuable source of computational and experimental data information and references for seal rotor dynamic characteristics. Childs reviewed the literature based on different seal geometries with different operating parameters. Swanson and Kirk (1997) carried out a survey of the experimental research on the static and/or dynamic characteristics of fixed geometry, hydrodynamic journal bearings, and reported the type(s) of bearing, size of bearing(s) and range of parameters measured in each work. Recently, Tiwari et al. (2004) have provided a comprehensive survey of the RDPs of bearings, with major emphasis especially on hydrodynamic bearings, with cursory mention of rotary seals.

The present literature survey is aimed at a review of experimental methods for the determination of the RDPs of seals in rotor-bearing seal systems, and will hopefully be useful to both practicing engineers and to the researchers in this field. For the practicing engineer, guidance is offered for the simple experimental determination of these parameters with associated uncertainty, whilst researchers may appreciate the diverse methods available and the discussion of their limitations so as to develop improved methods. The review has been presented in accordance with different types of seal geometry (i.e. plain annular seals, labyrinth seals, helically grooved seals, hole and triangular patterns, honeycomb seals, etc.) with some overlap (hybrid seals) among them. A chronological summary of this literature has been presented in tabular form (Table 1) and for brevity this information is not referred to again in the text.

2. Plain Annular Seals

In this section, we review the experimental study related to RDP estimation of straight, tapered, and long plain annular seals. Black and Jenssen (1969/70) presented experimental results for the stiffness of long plain seals to show the effect of the length-to-diameter ratio (*L/D*). Falco et al. (1984) obtained the equivalent stiffness and damping coefficients of plain fluid-film seals for constant radial clearance and with different values of *L/D* ratio by using two shakers placed at 120° apart (Figure 8). A torsiometer was used to evaluate the power dissipated by the seal.

Nordmann and Massmann (1984) estimated the RDPs of annular turbulent seals by using the impact hammer method. For tapered annular seals, Childs and Dressman (1985), using the test apparatus and facility developed by Childs and Kim (1985), observed that with an increase in taper angle while the direct stiffness and leakage increased, the remaining RDPs decreased. The results were compared with their own numerical results and those of Fleming (1980). Childs et al. (1986) developed a test apparatus to determine the RDPs of annular gas seals which had the following features: a maximum rotor speed of 8000 rpm, hydraulic shakers for excitation, and an inlet guide vane arrangement for controlling the inlet tangential velocity. Reaction forces exerted on the stator were measured by load cells that support the stator in the test section housing (Figure 9).

Nelson et al. (1986) used the experimental facility provided by Childs et al. (1986) to measure the leakage and to estimate the RDPs of constant-clearance and convergent-tapered annular gas seals in the shaft-centered position. The results were compared with their theoretical work (Nelson, 1984). It was observed that optimally tapered seals would have significantly larger direct stiffness than straight seals, and pre-rotation of the fluid yielded a large increase in direct stiffness.

Dynamic fluid reaction forces and moments of a long annular pump seal were experimentally estimated by Kanemori and Iwatsubo (1992). In the experimental setup, the outer cylinder (stator) was fixed with load cells and the rotor was independently driven by two motors to realize the spinning and whirling motions. Fluid forces were directly measured with load cells and a Pitot tube was used at the seal inlet to measure the circumferential flow velocity. Two pressure transducers were mounted on the stator to measure the fluid-film pressure fields in the seal clearance. The spinning velocity was measured using a pulse-generating tip attached to the rotor and a photo-interrupter. Experiments were conducted at various rotor speeds, whirling speeds, and with different pressure drops across the long seal to find the RDPs. These were then compared with Childs's theory (Childs, 1982) and found to be compatible. Direct stiffness and damping coefficients were mainly dependent and increased with pressure drop (inlet to outlet to the seal). The effect of pressure drops on the direct added-mass and cross-coupled damping coefficients was low.

Kaneko et al. (1998) experimentally investigated the static and dynamic characteristics for annular plain seals with porous materials applied to the seal surface using the same experimental setup as Kanemori and Iwatsubo (1992). They obtained dynamic forces by measuring fluid-pressure distributions circumferentially and axially in the seal clearance. Experimental results have shown that annular plain seals with porous materials have higher leakage flow rate (increase of approximately 30%), higher direct stiffness coefficients (four to six times) and smaller cross-coupled stiffness and direct damping coefficients (decrease of approximately 30%) than conventional annular plain seals with solid surfaces. The larger direct stiffness coefficients for the porous seals yielded larger radial reaction forces for a small concentric whirling motion, which would contribute to rotor stability.

A discrete-time domain estimation technique was applied by Brown and Ismail (1992) to estimate the RDPs of pump annular seals. In the test rig, water entered the stator at the mid-plane and discharged axially through a pair of annular seals. A seal model with 10 linearized coefficients was assumed and sampled input–output data obtained on a full-scale test rig facility were processed digitally to yield estimates of the coefficients as well as confidence bounds. They used a least-squares estimation procedure based on single value decomposition (SVD). The estimated coefficients were compared to those obtained from Black's theoretical model (Black and Jenssen, 1969/70; Black, 1979) for short seals with inlet swirl velocity and the seal length effects. Experimental estimation of the RDPs of long annular pump seals was presented by Brown and Ismail (1994). The inlet swirl magnitude was modified by a face-plate with a number of radial grooves on the inlet side of the annular seal. When compared with theoretical results, it was observed that experimental direct stiffness values were higher, cross-stiffness coefficients were lower at high axial Reynolds number, and the direct damping was in good agreement at low values of axial Reynolds number but the agreement was poor at higher values. Ismail and Brown (1996) presented the experimental estimation of the RDPs of long pump annular seals with deep radial grooves. It was observed that the cross-coupled stiffness and direct damping magnitudes were overestimated while the direct stiffness was underestimated. Brown et al. (1996) tested a pair of bronze plain annular seals and Ismail and Brown (1998) carried out an experiment for liquid long annular seals and compared their results with the theoretical work of Black (1971), Black et al. (1981), and Childs and Kim (1985). Brown et al. (1996) and Ismail and Brown (1998) compared the RDPs obtained with an analytical method for plain annular seals from linear bearing theory results. They found that the direct stiffness coefficients were underpredicted by the theory by about 20–30% and were insensitive to swirl reductions. The measured direct damping coefficients showed agreement with the theory at low axial Reynolds number only and were found to be insensitive to shaft speed, flow rate, and whirl reductions.

Alexander et al. (1995) investigated the effects of speeds, inlet pressures, pressure ratios, fluid pre-rotations, and eccentricities on the RDPs of a smooth gas seal using the test facility developed by Childs et al. (1986). Experimental results have shown that the direct stiffness decreases significantly, while the direct damping and cross-coupled stiffness increase with increasing eccentricity. Experimental results were compared to the theoretical analysis by Yang (1993). The theory (Yang, 1993) overpredicted direct stiffness, failed to indicate the decrease in the direct stiffness that occurred with increasing eccentricity, and incorrectly predicted the direct stiffness with changing pressure ratio. Also, the direct damping was substantially underpredicted for low pre-swirl values and low supply pressures, but predictions improved as either of these parameters increased.

An annular gas seal test stand was developed by modifying the hydrostatic bearing rig (HBR) used to test hybrid hydrostatic–hydrodynamic bearings (Childs and Hale, 1994). The apparatus could operate at a maximum speed of 29,800 rpm and accommodated seals of diameters up to 114.3 mm. Marquette et al. (1997) presented data for leakages and RDPs of a high-speed plain-annular seal at the centered and eccentric positions. It was observed that leakage flow rate increased slightly with an increase in the eccentric ratio, increased with an increase in the pressure drop, and decreased with an increase in the running speed. They reported agreement between experimental and theoretical results (San Andrés, 1991) in the centered position, even for direct inertia terms. However, RDPs were more sensitive to changes in eccentricity than predicted theoretically. Darden et al. (1999) developed a test rig and facility to obtain RDPs for a variety of high Reynolds number annular seals. They presented measurement techniques and an estimation method to obtain the RDPs. They found RDPs in agreement with theory (Padavala et al., 1993) for smooth annular seals. Lindsey and Childs (2000) compared experimental results with theoretical predictions using the Moody friction-factor model (Childs, 1993) for the turbulent flow, short, smooth annular seals with converging and diverging axial taper. Results showed that the direct stiffness generally increased with converging axial taper and decreased with diverging axial taper. The reduction in the direct stiffness in moving from the constant-clearance seal to the slightly convergent case was not predicted by the theory. Direct damping and cross-coupled stiffnesses were shown to decrease with increasing convergent or divergent taper. Measured damping values increased with an increase in running speeds and decreasing average clearances. The theory consistently underpredicted leakage in the range of 10–30%. The accuracy of theoretical predictions for the leakage and RDPs was not influenced by running speed. Replacing the pitch-stabilizing cables with rods increased the pitching motion natural frequency substantially and eliminated the problem of pitching at the zero running speed.

Dawson et al. (2002) estimated the RDPs and leakage characteristics of a pair of identical annular gas seals with a back-to-back arrangement inside the stator. Efforts to minimize transducer and instrumentation uncertainties were observed carefully by calibrating the displacement and pressure transducers, thermocouples, and flow meters before operation in the modified AGSTS.

3. Labyrinth Seals

In this section, we carry out a review of the RDP estimation of labyrinth seals. Wright (1978, 1983) described an apparatus for the accurate measurement of labyrinth seal forces on a whirling rotor model. The steam-excited whirl of a high-pressure turbine rotor was caused by the shroud and shaft labyrinth seal forces and by flow forces on the turbine blades. The effects of system parameters on the whirl excitation constant (whirl force/whirl amplitude) and the radial stiffness of a seal model were obtained. It was observed that the positive backward whirl excitation constant of the diverging seal was proportional to the pressure drop and was independent of the backpressure up to the transition pressure drop. At higher-pressure drop, it increased linearly but less rapidly with the pressure drop, and this increased with the backpressure. The forward whirl excitation constant of the diverging seal model was negative. A method was presented for predicting the net seal and blade-row excitation constant that would cause the self-excited whirl of rotors having specified shaft and bearing parameters.

Childs and Scharrer (1986, 1988) used the experimental test facility developed by Childs et al. (1986) to estimate the RDPs of the teeth-on-rotor and teeth-on-stator labyrinth gas seals. Childs and Scharrer (1986) estimated direct damping coefficients for different seal configurations, and observed that the stiffness and damping coefficients were insensitive to the rotor speed, very sensitive to the inlet tangential velocity, and increased with an increase in the inlet pressure. Also, they observed that the teeth-on-stator seal was more stable than the teeth-on-rotor seal for the positive inlet tangential velocity. Childs and Scharrer (1988) compared their experimental results with the theoretical work of Scharrer (1988). It was observed that the theory accurately predicted the cross-coupled stiffness for both seal configurations and showed improvement in the prediction of the direct damping for the teeth-on-rotor seal; however, the theory failed to predict a decrease in the direct damping coefficient for an increase in the radial clearance for the teeth-on-stator seal.

Using the experimental setup based on Nordmann and Massmann (1984), Kim and Lee (1994) presented RDPs and leakage for three annular seals: smooth, hole-pattern (damper), and labyrinth. The labyrinth seals used an antiswirl self-injection mechanism to yield significant improvement in whirl frequency ratios as compared to smooth and hole-pattern seals. It was observed that an optimum antiswirl self-injection seal, which used a labyrinth stator surface with anti-axial flow injections, showed significant improvement in the whirl frequency ratio as compared to a hole-pattern seal, while showing moderate leakage performances.

A labyrinth gas seal (TAMSEAL) developed by Vance and Li (1996) was studied in both non-rotating and rotating tests and it was observed experimentally that it had 100 times more direct damping than the conventional bladed seal. The latter seal had blocked swirl of the working fluid, which was destabilizing the rotor. The leakage rate of the TAMSEAL was higher than the conventional seal at the same clearance; however, large reductions in vibrations and whirl amplitudes suggested that the TAMSEAL could be operated with smaller clearances than conventional labyrinth seals. Test results from a non-rotating apparatus were reported by Vance and Schultz (1993).

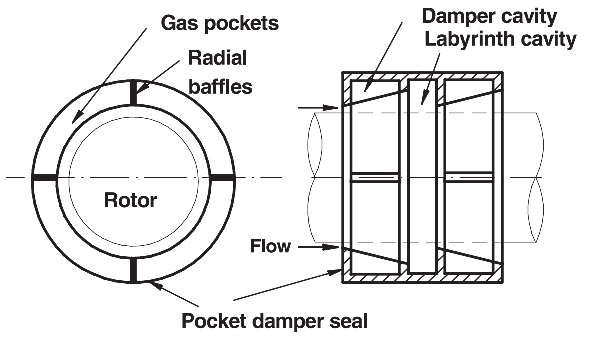

Figure 10. Geometry of a four-blade, two-four pocket damper seal (Li et al., 2000).

Ransom et al. (1999) identified the stiffness and damping force coefficients of a two-blade, tooth-on-stator labyrinth seal with the diverging clearance and its modified version as a four-pocket damper seal. In the test rig, a load gun was used to give impacts in the *X* and *Y* directions to the seal housing and induced its dynamic motion. Four displacement sensors and pressure sensors were fastened to the housing cap, and two accelerometers were mounted on the housing sides. It was observed that the four-pocket gas damper seal had large (positive) direct damping coefficients and relatively small (negative) direct stiffness coefficients while the two-bladed labyrinth seal exhibited positive direct stiffness and negative damping force coefficients. However, the leakage performance of both seals was nearly identical. Li et al. (1999b, 2000) used the test facility developed by Ransom et al. (1999) and demonstrated that multiple-pocket gas damper seals offered enough direct damping coefficients to effectively eliminate subsynchronous rotor vibrations and reduced amplitudes of rotor imbalance responses. The bulk-flow model and experiments by Li et al. (1999b) indicated that the seal direct stiffness and damping force coefficients were insensitive to journal speeds while the cross-coupled stiffness increased slightly and force coefficients of multiple-pocket gas damper seals were also functions of the rotor excitation frequency. Li et al. (2000) presented experimental RDPs and leakage for a four-blade, two four-pocket gas damper seals (Figure 10) using the test rig made by Ransom et al. (1999) and compared to predictions based on a one control volume bulk-flow model (Li et al., 1999a). It was observed that both measurements and predictions agreed well and showed that the seal direct stiffness and damping coefficients were proportional to the inlet to exit pressure ratio and insensitive to rotor speed.

Kwanka (2000) obtained seal RDPs with a stepped-labyrinth seal and compared these with a tooth-on-stator labyrinth seal. It was observed that the cross-coupled stiffness showed almost linear behavior (a usual) dependence on swirl conditions at the entrance of seal. A higher-pressure difference showed higher stiffness values. Dependences of the direct damping on the pressure difference and the swirl were not clear. The stepped-labyrinth seal generated a positive direct stiffness (a stabilizing effect). Wagner (2001) used a test rig for high pressures (Wagner and Steff, 1996) to estimate labyrinth seal RDPs. Forces were measured directly via active magnetic bearings. This allowed direct calculation of transfer functions without force transducers. From these transfer functions, seal RDPs were extracted. They carried out experiments for the straight-through, stepped and staggered labyrinth and honeycomb seals with abradable rotor coatings and various swirl brakes to reduce the inlet tangential velocity, which could substantially reduce or eliminate k_c.

4. Helically Grooved Seals

In this section we review the experimental estimation of helically grooved seal RDPs. Kanki and Kawakami (1984) investigated the static and dynamic characteristics of pump annular cylindrical and screw-grooved seals for a wide range of circumferential and axial Reynolds numbers and eccentricities. They used rubber air-bellows (with static pressure) to support and two hydraulic actuators to excite the seal housing. Using the test facility of Childs and Kim (1985), Childs et al. (1990b) experimentally observed that helically grooved stators leaked more than smooth seals for helix angles greater than 30°, and that the effective direct stiffness of seals first decreased and then increased with increasing helix angles. Also, contrary to theoretical predictions (Kim and Childs, 1987), the effective net damping was relatively insensitive to changes in helix angles.

Childs and Gansle (1996) presented RDPs and leakage test results for three grooved seals with helix angles of 0°, 15°, and 30° against inlet fluid pre-rotation using the test rig developed by Childs et al. (1986) with modifications made by Pelletti and Childs (1991). Results showed that increasing the helix angle yielded a progressive reduction in the cross-coupled stiffness coefficient k_c and progressive increase in leakage. Helically grooved seals consistently yielded negative cross-coupled stiffness coefficients for non-pre-rotated inlet flows. The comparison between the helically grooved and honeycomb-stator seals showed that the former had reduced (negative) whirl frequency ratios for non-pre-rotated flows; however, they were no better than the latter for elevated fluid pre-rotation. For 15° and 30° of helix grooves of the helically grooved seals, leakage was about 1.6 and 2.2 times, respectively, as much as the honeycomb-stator seals.

5. Circular-Hole or Triangular Pattern Seals

In this section, we review the experimental estimation of RDPs for seals with different types of surface pattern. Childs and Kim (1985) presented test results for the smooth-finish, knurled-indentation, diamond-grid, and round-hole-pattern stator configurations. Axially spaced pressure transducers were provided to measure transient pressure fields. While comparing with their own theory, Childs and Kim (1985) observed that the predicted net damping increased for non-smooth seals. Round-hole-pattern stators yielded the highest net damping and lowest leakage. The seal was substantially stiffer than the theoretical prediction, but the theory reasonably predicted the net damping. It was observed that the maximum net damping was achieved by (a) a hole pattern, which takes up about 34% of the surface area, and (b) hole depths, which were about three times the radial clearances. When compared with a smooth seal, the optimum configuration increased the net damping by 37%, while reducing the leakage by 46% and the direct stiffness by 23%.

Childs and Garcia (1987) obtained the direct force coefficients for saw-tooth pattern damper seals. It was found experimentally that saw-tooth pattern seals showed more damping than smooth seals but less than the round-hole-pattern seals. The stiffnesses of the saw-tooth and round-hole-pattern seals were comparable. The leakage of maximum-damping configurations was greater for saw-tooth pattern seals than round-hole-pattern seals; however, the leakages for both types of seals were substantially less than smooth seals. Iwatsubo et al. (1990) investigated experimentally the static and dynamic characteristics of two types of triangular-hole-pattern seals, which had the same hollow surface patterns but different hollow depths. Test results showed that leakages of triangular-hole-pattern seals were much smaller than those of smooth seals, and for a given surface pattern, there was an optimum hollow depth at which the seal yielded the minimum leakage. Triangular-hole-pattern seals could effectively restrict the pre-swirl velocity and reduce the circumferential velocity, thus ensuring better stabilizing performance.

Childs et al. (1990c) found leakage rates, axial pressure gradients, friction factors, and RDPs for round-hole-pattern seals with no intentional pre-rotation. It was observed that the leakage of hole-pattern-stator seals was approximately one-third less than smooth seals for the same clearances, and had approximately the same damping and about 20% lower stiffness. Unlike earlier tests (Childs and Kim, 1986) variations in hole depths to radial clearance ratios showed no clear optimum dimensions with respect to damping.

Childs and Fayolle (1999) studied two liquid annular hole-pattern roughened stator seals using modified AGSTS (Marquette et al., 1997) and observed that test results were consistent with expectations with regard to the reduction of cross-coupled stiffness coefficients due to the stator roughness. However, the measured direct stiffness coefficients were unexpectedly low. However, a theoretical model (Nelson and Nguyen, 1987) for RDPs incorporating the friction factor data predicted a substantial loss in the direct stiffness, and could not explain very low (or negative) values that were measured.

Darden et al. (2001) described the effect of pre-swirl on the stabilizing capability of both the damper (with a hole density of 0.35) and smooth seals using the test rig and data reduction techniques provided by Darden et al. (1999). Centered seal results were presented for both the smooth annular and damper seals for a range of seal pressure drops, shaft rotational speeds, and two levels of inlet fluid pre-swirls (which was achieved by a shaft that incorporated 10 radial fins located just upstream of the seal entrance). It was observed that in the low pre-swirl testing, good agreement was obtained for the direct stiffness of the smooth seal for both cases of high and low pressures. The direct stiffness results for the damper seal indicated that the theory (Padavala et al., 1993) overpredicted stiffness coefficients by approximately 50%. The dimensionless cross-coupled stiffness for the smooth seal was underpredicted at higher speeds. The damper seal cross-coupled stiffness curves indicated that the theory overpredicted by as much as 15%. Good agreement between experimental results and theoretical predictions was obtained for the smooth seal direct damping for both high and low seal pressure drops. In the high pre-swirl testing, the direct stiffness for the smooth seal was overpredicted by approximately 20–30%. The direct stiffness for the damper seal was overpredicted again by 50%. The smooth seal results indicated that the theory overpredicted the cross-coupled stiffness by roughly 10%.

Holt and Childs (2002) obtained RDPs for two hole-pattern-stator seals and one smooth-bore seal using the test rig developed by Childs and Hale (1994), and compared test results with the two control-volume theoretical model (Kleynhans and Childs, 1997). It was observed that hole-pattern seals exhibit frequency-dependent RDPs as predicted by the theory. The measured effective direct damping and the leakage were close to those predicted theoretically; however, the effective direct stiffness was underpredicted in all cases. Also, RDP predictions improved with increasing pressure ratio and the leakage decreased as cell depths increased.

Childs and Wade (2004) obtained RDP results for an annular gas seal using a smooth rotor and a hole-pattern roughness stator using the basic test facility developed by Childs and Hale (1994) for three pressure ratios, speeds, and pre-swirl ratios. It was observed that theoretical predictions based on the two-control volume bulk-flow model (Kleynhans and Childs, 1997) agreed with measurements very well at high pre-swirl values, but underpredicted the direct damping and cross-coupled stiffness coefficients. Agreement between measurements and predictions was significantly better at the lower radial clearance (0.10 mm) than at higher clearance (0.20 mm). They also estimated the stiffness and damping arising from the exit seals, hose connections, etc. To account for these additional elements, "baseline" tests were conducted without the test seals. These tests were conducted at reduced supply pressures to match the "real test" backpressures experienced by the backpressure seals.

6. Honeycomb Seals

In this section, we review RDP estimation of honeycomb seals. Childs et al. (1991) modified the basic test rig developed by Childs et al. (1986) with the high-pressure supply, the pre-swirl arrangement, and swept-sine excitations. Hawkins et al. (1989) obtained the experimental measurements for RDPs of a teeth-on-rotor labyrinth seal with a honeycomb stator for the primary variables (i.e. inlet circumferential velocities, inlet pressures, rotor speeds, and seal clearances) and compared the results with the experimental results of Childs and Scharrer (1988) and the theoretical results (Scharrer, 1988). It was observed experimentally that the honeycomb-stator configuration was more stable than the smooth-stator configuration at low speeds, but the stator surface did not affect stability at high rotor speeds.

Childs et al. (1989) presented test results for the leakage and RDPs for honeycomb seals of different cell depths and diameters. The RDPs presented for a range of honeycomb cell dimensions showed considerable sensitivity to the changes in cell dimensions. Comparisons of the test data for honeycomb seals with labyrinth and smooth annular seals showed that the honeycomb seal had the best sealing (minimum leakage) performance, followed in order by the labyrinth and smooth seals. For pre-rotated fluids entering the seal, in the direction of shaft rotation, the honeycomb seal had the best rotor dynamic stability, followed in order by the labyrinth and smooth seals. For no pre-rotation, or fluid pre-rotation against shaft rotation, the labyrinth seal had the best rotor dynamic stability, followed in order by the smooth and honeycomb seals. Elrod et al. (1989) developed a friction-factor model for an annular gas seal analysis similar to that of Nelson (1984). Theoretical and experimental predictions for smooth-stator/smooth-rotor and honeycomb-stator/smooth-rotor seals were compared with experimental results (Childs et al., 1989) and it was observed that the model predicted the leakage and direct damping well. However, it overpredicted the dependence of the cross-coupled stiffness on the fluid pre-rotation and poorly predicted the direct stiffness. Childs et al. (1990a) obtained test results of honeycomb annular seals for different pressure ratios across the seal with a fixed supply pressure and compared them with the theory of Elrod et al. (1990). It was observed that the whirl-frequency ratio improved as the pressure ratio increased and was very sensitive to changes in cell dimensions with improved stability for larger cell sizes. Correlation between theory and experiment was significantly worse for these seals than earlier tests (Childs et al, 1989) of honeycomb seals, due to the inadequacy of the fluid friction model in the analysis (Elrod et al., 1990).

Childs and Ramsey (1991) obtained experimental RDP results of a seal model (i.e. in the space shuttle main engine under a project on "alternate turbopump development (ATD)" for the high-pressure fuel turbopump (HPFTP)) for three fluid pre-rotation cases and for four pressure ratios with and without swirl brakes, and they compared the RDPs with the theoretical results (Scharrer, 1988). Test results demonstrated a pronounced favorable influence of the swirl brake in reducing the seal destabilizing forces. Without the swirl brake, the cross-coupled stiffness (k_c) increased monotonically with the increase in the inlet tangential velocity. With the swirl brake, k_c tends either to remain constant or to decrease with the increase in tangential velocity. The direct damping either increased or remained relatively constant when the swirl brake was introduced; however, the direct stiffness was relatively unchanged. No measurable differences in leakage were detected for the seal with and without the swirl brake. Childs et al. (1991) presented RDPs from the test of the turbine interstage seal for the high-pressure oxygen turbopump (HPOTP) with two types of swirl brakes: conventional swirl brake (designed by Rocketdyne) and alternate swirl brake (aerodynamically designed by them) for the same fluid pre-rotation cases and operating conditions. It was observed that the alternate swirl brake consistently outperformed the conventional swirl brake in terms of stability performances, and yielded negative whirl frequency ratio values in comparison to positive values for the conventional design, but no change in the leakage performance.

Childs and Kleynhans (1992) extended the work of Childs et al. (1989) and presented the effects of inlet fluid pre-swirls, rotor speeds, inlet pressures, pressure ratios across the seal, seal clearances, and honeycomb cell widths on experimental RDPs and the leakage of the short (L/D = 1/6) honeycomb and smooth annular pressure gas seals. Results showed that decreasing the honeycomb cell width reduced the leakage. Rotor dynamically, shorter honeycomb seals did not perform as favorably as longer seals (L/D = 1/3) when compared with the labyrinth and smooth geometries. The magnitude of RDPs and whirl frequency ratios increased while decreasing seal clearances and absolute pressure ratios. High sensitivity to the inlet fluid pre-swirl suggested that short seals required an effective swirl brake to enhance rotor dynamic stability. Dawson and Childs (2002) obtained results from tests conducted using a experimental test facility (Dawson et al., 2002) to estimate RDPs and to measure the leakage of the smooth and honeycomb straight-bore annular gas seals; they compared the test results with the two-control volume model of Kleynhans and Childs (1997). They found that honeycomb seals did not fit well with the conventional frequency independent model of smooth annular gas seals. Soto and Childs (1999) presented test results using the test rig developed by Childs et al. (1986) for (i) a labyrinth seal with and without shunt injection and (ii) a honeycomb seal. It was observed from the results that, while considering the effective damping, the labyrinth seal with injection against rotation was better than the honeycomb seal when the pressure ratio across the seal was less than 0.45 and honeycomb seal was better when the pressure ratio was greater than 0.45.

Kwanka (2001) developed an estimation procedure based on the stability behavior of a flexible rotor to determine the RDPs. He tested seals with smooth/honeycomb stator and teeth-on-rotor geometries with or without swirl brakes, using the test apparatus described in Kwanka (2000). It was found that seals with labyrinth rotor and honeycomb stator could not always be recommended due to the small direct damping. The use of a honeycomb seal in combination with swirl brakes optimized (minimized) both the leakage and the rotordynamic instability. Nielsen et al. (2001) presented experimental and theoretical data for seals (labyrinth-rotor/honeycomb-stator) with two interchangeable swirl brakes, which were designed in connection with a research program (see Childs and Ramsey, 1991) for four independent variables: supply pressures, pressure ratios, rotor speeds, and inlet circumferential velocities. Numerical simulations were made with the three-dimensional Navier–Stokes solver CFX-TAS-Cflow from AEA Technology (1999), which is a general purpose computational fluid dynamics code able to deal with complex three-dimensional flows. It was observed that the two interchangeable swirl brake designs considered were effective in terms of reducing the seal inlet swirl, and thereby improving rotor dynamic stability due to a very significant decrease in the cross-coupled stiffness. Weatherwax and Childs (2003) obtained test results for a honeycomb-stator/smooth-rotor annular seal for eccentricity ratios up to 0.5 using the basic test facility described in Childs and Hale (1994). They compared the results with a two-control volume model for honeycomb seals developed by San Andrés (1991). It was observed that either leakage or RDPs have minimal sensitivity to changes in the eccentricity ratio and theoretical predictions agreed with experiments.

Honeycomb damper seals with the convergent-tapered clearance were developed by Kaneko et al. (2003) to improve static and dynamic characteristics of liquid annular seals employed in pumps. Their characteristics were experimentally investigated using the basic test facility developed by Kanemori and Iwatsubo (1992). They compared their experimental results with those for the straight-annular seal and the stator-honeycomb-pattern seal. Experimental results showed that the convergent-tapered damper seals as well as the straight damper seal had lower leakage flow rates and cross-coupled stiffness coefficients, and larger main damping coefficients than the straight smooth seal. This resulted in larger effective damping coefficients, and these results were mainly due to surface roughness (honeycomb pattern) in the seal stator. Due to the convergent-tapered clearance with damper, the seal had larger main stiffness coefficients than others. The convergent-tapered damper seals had better seal characteristics (i.e. decreasing the leakage and improving the rotor stability capacity) than the conventional straight-smooth and the straight-damper seals with the same roughness pattern.

7. Brush and Hybrid Seals

In this section we review the literature on the dynamic characteristics of brush and hybrid seals. Suzuki et al. (1986) presented test results (leakage) of a face seal and a floating-ring seal for a liquid hydrogen turbopump for high speed and high pressure. Conner and Childs (1993) obtained experimental RDPs for a four-stage brush seal for different inlet pressures, pressure ratios, shaft speeds, fluid pre-rotations, and seal spacings. It was observed that the direct damping slightly increased with running speeds; otherwise, the RDPs are relatively insensitive to changes in test parameters. The cross-coupled stiffness for the present case was generally unchanged by increasing inlet tangential velocities to seals, in contrast to conventional labyrinth seals. Comparison of test results for the four-stage brush seal with an eight-cavity labyrinth seal showed a high stability for the brush seal.

Pocket damper seals were shown to provide a remarkable amount of direct damping to attenuate vibration in turbomachinery, but they generally leaked more than conventional labyrinth seals if both seals had the same minimum clearance. Conversely, brush seals allow less than half the leakage of labyrinth seals, but have no significant amount of damping. Laos et al. (2000) presented test results of the hybrid brush/pocket damper seal (Figure 11) that combines low leakage and high damping. They modified a computer code (based

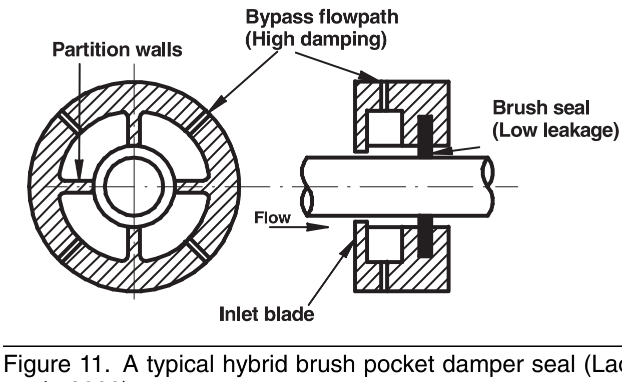

Figure 11. A typical hybrid brush pocket damper seal (Laos et al., 2000).

on Vance and Schultz, 1993) written for the original pocket damper seal to include the brush element. Results from the computer code and experiments indicated that the hybrid seal had less leakage than the labyrinth seal and had more damping than the original pocket damper seal.

8. Uncertainty Analysis

Uncertainty of the test data is a result of the individual uncertainties inherent with each instrument. Most researchers (Childs and Scharrer, 1986, 1988; Childs et al., 1989, 1990a, 1991; Hawkins et al., 1989; Childs and Ramsey, 1991; Childs and Kleynhans, 1992; Kurtin et al., 1993; Alexander et al. 1995; Childs and Gansle, 1996; Nielsen et al., 2001) have used the method described by Holman (1978) to estimate the uncertainty in the RDPs. The method is briefly stated as follows. Let the results R (e.g. RDPs) be a given function of the independent variables $x_1, x_2, \ldots, x_n$ (e.g. rotor speed, inlet pressure, pressure drop, diameter, length, clearance, temperature, force, excitation frequency, displacement, acceleration, etc.). Thus,

$$R = R(x_1, x_2, \ldots, x_n). \tag{7}$$

Let w_R be the uncertainty in the result and let $w_1, w_2, \ldots, w_n$ be the uncertainties in the independent variables. Then the uncertainty in the result is given as

$$w_R = \left[\left(\frac{\partial R}{\partial x_1}w_1\right)^2 + \left(\frac{\partial R}{\partial x_2}w_2\right)^2 + \ldots + \left(\frac{\partial R}{\partial x_n}w_n\right)^2\right]^{1/2} \tag{8}$$

with

$$\frac{\partial R}{\partial x_1} \approx \frac{R(x_1+\Delta x_1) - R(x_1)}{\Delta x_1};\quad \frac{\partial R}{\partial x_2} \approx \frac{R(x_2+\Delta x_2) - R(x_2)}{\Delta x_2};\ldots \tag{9}$$

where $\Delta x_1, \Delta x_2, \ldots, \Delta x_n$ are the small perturbations of the independent variables. It should be noted that the uncertainty propagation in the results w_R predicted by equation (8) depends on the squares of the uncertainties in the independent variables w_n. This means that if the uncertainty in one variable is significantly larger than the uncertainties in the other variables, then it is the largest uncertainty that predominates and the other may probably be negligible. The relative magnitude of uncertainties is evident when one considers the design of an experiment, procurement of instrumentations, etc. Most researchers have found the effect of uncertainty measurement in the force, excitation frequency, and displacement measurements on the stiffness, damping and added-mass coefficients.

According to Childs and Ramsey (1991), the principal source of uncertainty in the resultant force measurement was the acceleration measurement for the stator. Although more sensitive accelerometers are available, they cannot generally be used when testing honeycomb seals, because high-frequency acceleration spikes were frequently seen with these seals, presumably because of Helmholtz acoustic excitation of honeycomb cavities. Kanemori and Iwatsubo (1992), Kaneko et al. (1998, 2003), and Childs and Fayolle (1999) carried out uncertainty analysis using methods established by ANSI/ASME (1986). Childs and Wade (2004) obtained the uncertainty of RDPs for variation of excitation frequency. They calculated the test uncertainty at each frequency as the square root of the sum of squares of baseline uncertainty and seal test uncertainty at each frequency. Details of the authors who performed the uncertainty analysis of the estimated RDPs are mentioned in Table 1.

9. General Remarks and Future Directions

1. For the last three decades there has been increased concern over seal-induced instability, and hence there has been an exponential increase in research on the RDPs of seals. Theoretical and experimental estimations of the RDPs of seals are much more complicated than for bearings.
2. The cross-coupled stiffness force (e.g. $k_{xy}\Delta y$) arises due to fluid rotation within the seal clearance and acts in opposition to the direct damping force (e.g. $c_{xx}\Delta\dot{x}$) to destabilize the rotor. Hence, to improve the rotor stability, steps should be taken to reduce the net fluid rotation within the seal by reducing the cross-coupled stiffness.
3. Small direct stiffness coefficients can be undesirable from the point of view of rotor dynamics, since it may decrease the rotor critical speed. Optimally tapered seals have significantly larger direct stiffness than straight seals.
4. Grooving on stator/rotor significantly reduces stiffness and damping effects, possibly as much as 80% reduction with wide and deep grooves. Having grooves on seal stator (teeth-on-stator seal) is rotor dynamically more stable than having grooves on the rotor (teeth-on-rotor seal).
5. In labyrinth/honeycomb seals, the leak flow rate is less than that in smooth annular seals. In brush seals, leakage is much less compared with labyrinth/honeycomb seals. The major improvement provided by these labyrinth/honeycomb and brush seals is a significant reduction in tangential flow velocity within the seal, which significantly reduces the destabilizing cross-coupled stiffness effect. However, the bristle motion characterized by circumferentially traveling waves occurring in the bristles leads to their premature wear-out. Labyrinth/honeycomb seals also yield a reduction in main stiffness coefficients.
6. Honeycomb seals are used to eliminate rotor dynamic instabilities in compressor or turbine applications. The stability measured by the whirl frequency ratio improves as the pressure ratio increases. The stability is shown to be very sensitive to changes in cell dimensions with improved stability for the larger cell sizes.
7. Swirl brakes in the upstream seal, which reduce the inlet tangential velocity, could substantially reduce or eliminate the cross-coupled stiffness coefficient, k_c. To improve the efficiency and stability margin of the pumps, it is generally required that annular seals reduce k_c and the leakage flow rate and increase in the direct-stiffness (k_d) and direct-damping coefficients (c_d).
8. The hybrid brush pocket damper seal is a combination of pocket damper and brush seals, which are mainly for high damping and low leakage, respectively. Therefore, this seal combines high damping with low leakage.

9. The geometry of rotary seals is quite complex and it leads to difficulty in modeling and analyzing seals by theoretical and computational methods. Analytical models of rotary seals are multifaceted and still under improvement with new seal designs. Analytical and computational analyses methods of seals are tedious and are still under development.
10. Various geometric parameters of seals affect RDPs, such as diameters, clearances and lengths of seals, hole diameters, density of holes and hole depths in hole-pattern seals, and other dimensions defining different pattern (honeycomb, triangular, etc.) seals etc. There is a need to develop new mathematical models of seals based on experiments to represent the behavior of rotor-bearing-seal systems.
11. Available experimental data resources on RDPs of seals can be used for only qualitative comparisons since the number of parameters affecting RDPs is large, and in several cases not all of these parameters are reported. Hence, there is a need for standardization of the data given in publications in the field of seal RDP estimation. Moreover, for maximum usefulness to analysts, the identified RDPs of seals should be documented in tabular form and equation coefficients for curve fits given along with the documentation of operating conditions. There is a need for raw/processed measured data to be made available and exchanged among the researchers in the field.
12. Experimental estimation of the RDPs of seals has been mainly obtained on dedicated test rigs under controlled excitations. The validation of the seal RDPs using data derived from actual machines in the actual operating environment (from excitations inherent in systems) is required. Synchronous unbalance responses, which can easily be generated and are present inherently in any rotor systems, should be exploited more for the estimation of RDPs along with the estimation of residual unbalances.
13. Frequency-domain methods are preferable in terms of the quantity of data to be handled/stored. The signal-to-noise ratio is found to be better for frequency-domain methods, and hence the estimation of the RDPs of seals is more reliable in the frequency domain. While using impact tests (multifrequency tests) it is necessary to remove the unbalance response from the signal, especially at higher speeds of operation. In multifrequency tests (either by using an exciter or impact hammer) it is assumed that the seal RDPs are independent of the frequency of excitation, which may not be true for all cases.
14. Theoretical, computational, and experimental error analysis of RDPs of seals should be presented as an integral part of all the estimates.
15. There is still a need for experimental work in the field of rotor dynamics to study the influence of seals and supports upon the rotor response, in particular for full-scale rotor systems. New experiments should be devised and more effective use of the available data needs to be made, especially with the inherent practical constraints for measurements and development of new estimation techniques.

Acknowledgment

RT gratefully acknowledges the encouragement given by Turbopump Group, Liquid Propulsion Systems Center, Indian Space Research Organization to carry out the present work.

References

Adams, M. L., 1987, *Rotating Machinery Vibration: From Analysis to Troubleshooting*, Marcel Dekker, New York.

Admas, M. L. Jr, 2001, *Rotating Machinery Vibration*, Marcel Dekker, New York.

AEA Technology, 1999, CFX-TASCflow User Documentation, Version 2.9.

Alexander, C. R., Childs, D. W., and Yang, Z., 1995, "Theory Versus Experiment for the Rotordynamic Characteristics of a Smooth Annular Gas Seal at Eccentric Positions," *ASME Journal of Tribology*, Vol. 117, No. 1, 148–152.

Alford, J. S., 1964, "Protection of Labyrinth Seals from Flexural Vibration," *ASME Journal of Engineering for Gas Turbines and Power*, Vol. 86, No. 2, 141–148.

Alford, J. S., 1965, "Protecting Turbomachinery from Self-Excited Rotor Whirl," *ASME Journal of Engineering for Gas Turbines and Power*, Vol. 87, No. 4, 333–344.

Allaire, P. E. and Flack, R. D., 1982, "Static and Dynamic Radial Forces on Centrifugal Impellers," presented at EPRI Pump Workshop, Toronto, Canada.

Allaire, P. E., Lee, C. C., and Gunter, E. J., 1978, "Dynamics of Short Eccentric Plain Seals with High Axial Reynolds Number," *Journal of Spacecraft*, No. 6, 341–347.

ANSI/ASME, 1986, "Measurement Uncertainty," *Supplement to Performance Test Codes, Instruments and Apparatus*, PTC 19.1-1985, Part I, ASME (Reconfirmed in 1990).

Arghir, M. and Frêne, J., 2004, "A Bulk-flow Analysis of Static and Dynamic Characteristics of Eccentric Circumferentially Grooved Liquid Annular Seals," *ASME Journal of Tribology*, Vol. 126, No. 2, 316–325.

Baheti, S. K. and Kirk, R. G., 1994, "Thermo-hydrodynamic Solution of Floating Ring Seals for High Pressure Compressors Using the Finite-element Method," *Tribology Transactions*, Vol. 37, No. 2, 336–346.

Baheti, S. K. and Kirk, R. G., 1995, "Finite Element Thermo-hydrodynamic Analysis of a Circumferentially Grooved Floating Oil Ring Seal," *Tribology Transactions*, Vol. 38, No. 1, 86–96.

Baheti, S. K. and Kirk, R. G., 1999, "Analysis of High Pressure Liquid Seal Ring Distortion and Stability Using Finite Element Methods," *Journal of Tribology*, Vol. 121, No. 4, 921–926.

Baheti, S. K., Ramesh, K., and Kirk, R. G., 1996, "Effect of Axially Grooved Oil Seals on the Leakage and Stability of a Centrifugal Compressor," *Tribology Transactions*, Vol. 39, No. 2, 398–406.

Benkert, H., and Wachter, J., 1980, "Flow Induced Spring Coefficients of Labyrinth Seals for Applications in Rotordynamics," *Proceedings of the 1st Workshop on Rotordynamic Instability Problems in High Performance Turbomachinery*, Texas A&M University, May 12-14, NASA CP 2133, pp.189-212.

Black, H. F., 1969, "Effects of Hydraulic Forces in Annular Pressure Seals on the Vibration of Centrifugal Pump Rotors," *Journal of Mechanical Engineering Science,* Vol. 11, No. 2.

Black, H. F., 1971, "Effects of High Pressure Ring Seals on the Pump Rotor Vibrations," *ASME* No. 71-WA/FF-38.

Black, H. F., 1979, "Effects of Fluid-filled Clearance Spaces on Centrifugal Pump and Submerged Motor Vibrations," in Proceedings of the 8th Turbomachinery Symposium, Gas Turbine Laboratories, Texas A&M University.

Black, H. and Jenssen, D., 1969/70, "Dynamic Hybrid Properties of Annular Pressure Seals," *Proceedings of IMechE*, *Journal of Mechanical Engineering*, Vol. 184, Part 3N, 92–100.

Black, H. L., Allaire, P. E., and Barrett, L. E., 1981, "Inlet Flow Swirl in Short Turbulent Seal Dynamics," in Proceedings of the 9th International Conference on Fluid Sealing, Leeewenhorst, the Netherlands, April 1–3.

Blasius, H., 1913, "Das Ahnlichkeitsgesetz bei Reibungsvorgangen in Flussigkeiten," Forschg. Arb Ing.-Wes., Heft 131, Berlin.

Brown, R. D. and Ismail, M., 1992, "Dynamic Characteristics of Long Annular Seals in Centrifugal Pumps," in Proceedings of the 5th

International Conference on Vibration in Rotating Machinery, IMechE, Bath, UK, No. C432/112, 315-324.

Brown, R. D. and Ismail, M., 1994, "Experimental Dynamic Coefficients of Long Annular Seals," in Seminar on Vibration in Fluid Machinery, IMechE, Mechanical Engineering Publications, London.

Brown, R. D., Ismail, M., Wilkinson, P., and Worden, K., 1996, "Estimation of Dynamic Coefficients in Fluid Films with Reference to Journal Bearings and Seals," in International Conference on Estimation in Engineering Systems, Swansea, UK, March.

Childs, D. W., 1982, "Rotordynamic Moment Coefficients for Finite Length Turbulent Seals," in Proceedings of the IFToMM Conference, Rome, Italy, September, 371–378.

Childs, D. W., 1983a, "Dynamic Analysis of Turbulent Annual Seals Based on Hirs Lubrication Equations," *ASME Journal of Lubrication Technology*, Vol. 105, No. 3, 429–436.

Childs, D. W., 1983b, "Finite Length Solutions for Rotordynamic Coefficients of Turbulent Annular Seals," *ASME Journal of Lubrication Technology*, Vol. 105, No. 3, 437–445.

Childs, D. W., 1993, *Turbomachinery Rotordynamics: Phenomena, Modeling and Analysis*, Wiley, New York.

Childs, D. W., and Dressman, J. B., 1985, "Convergent-tapered Annular Seals: Analysis and Testing for Rotordynamic Coefficients," *ASME Journal of Tribology*, Vol. 107, 307–317.

Childs, D. W. and Fayolle, P., 1999, "Test Results for Liquid "Damper" Seals using a Round-Hole Roughness Pattern for the Stators," *ASME Journal of Tribology*, Vol. 121, No. 1, 42–49.

Childs, D. W. and Gansle, A. J., 1996, "Experimental Leakage and Rotordynamic Results for Helically Grooved Annular Gas Seals," *ASME Journal of Engineering for Gas Turbines and Power*, Vol. 118, No. 2, 389–393.

Childs, D. W. and Garcia, F., 1987, "Test Results for Sawtooth-Pattern Damper Seals: Leakage and Rotordynamic Coefficients," *ASME Journal of Tribology*, Vol. 109, No. 1, 124–128.

Childs, D. and Hale, K., 1994, "Test Apparatus and Facility to Identify the Rotordynamic Coefficients of High-Speed Hydrostatic Bearings," *ASME Journal of Tribology*, Vol. 116, No. 2, 337–344.

Childs D. W., and Kim, C-H., 1985, "Analysis and Testing for Rotordynamic Coefficients of Turbulent Annual Seals with Different, Directionally Homogeneous Surface Roughness Treatment for Rotor and Stator Elements," *Transactions of the ASME Journal of Tribology*, Vol. 107, No. 3, 296–306.

Childs, D. W. and Kim, C. H., 1986, "Test Results for Round-Hole-Pattern Damper Seals: Optimum Configurations and Dimensions for Maximum Net Damping," *ASME Journal of Tribology*, Vol. 108, No. 4, 605–611.

Childs, D. W. and Kleynhans, G. F., 1992, "Experimental Rotordynamic and Leakage Results for Short (L/D = 1/6) honeycomb and smooth annular pressure seals," in Proceedings of the 5th International Conference on Vibrations in Rotating Machinery, IMechE, Bath, UK, No. C432/003, 305–309.

Childs, D. W. and Ramsey, C., 1991, "Seal-Rotordynamic-Coefficient Test Results for a Model SSME (Space Shuttle Main Engine) ATD (Alternate Turbopump Development)–HPFTP (High-Pressure Fuel Turbopump) Turbine Interstage Seal With and Without a Swirl Brake," *Transactions of the ASME Journal of Tribology*, Vol. 113, No. 1, 198–203.

Childs, D. W. and Scharrer, J. K., 1986, "Experimental Rotordynamic Coefficient Results for Teeth-on-Rotor and Teeth-on-Stator Labyrinth Gas Seals," *ASME Journal of Engineering for Gas Turbines and Power*, Vol. 108, No. 4, 599–604.

Childs, D. W. and Scharrer, J. K., 1988, "Theory Versus Experiment for the Rotordynamic Coefficient of Labyrinth Gas Seals: Part II – A Comparison to Experiment," *Transactions of the ASME Journal of Vibration, Acoustics, Stress and Reliability in Design*, Vol. 110, No. 3, 281–287.

Childs, D. and Wade, J., 2004, "Rotordynamic Coefficient and Leakage Characteristics for Hole-Pattern-Stator Annular Gas Seals – Measurements Versus Predictions," *ASME* Journal *of Tribology*, Vol. 126, No. 2, 326–333.

Childs, D., Nelson, C., Nicks, C., Scharrer, J., Elrod, D., and Hale, K., 1986, "Theory Versus Experiment for the Rotordynamic Coefficients of Annular Gas Seals: Part I – Test Facility and Apparatus," *ASME Journal of Tribology*, Vol. 108, 426–432.

Childs, D. W., Elrod, D., and Hale, K., 1989, "Annular Honeycomb Seals: Test Results for Leakage and Rotordynamic Coefficients; Comparison to Labyrinth and Smooth Configurations," *ASME Journal of Tribology*, Vol. 111, No. 2, 293–301.

Childs, D. W., Elrod, D., and Ramsey, C., 1990a, "Annular Honeycomb Seals: Additional Test Results for Leakage and Rotordynamic Coefficients," in Proceedings of the 3rd International Conference on Rotordynamics, IFToMM, Lyons, France, 303–306.

Childs, D. W., Nolan, S. A., and Kilgore, J. J., 1990b, "Test Results for Turbulent Annular Seals, Using Smooth Rotors and Helically Grooved Stators," *ASME Journal of Tribology*, Vol. 112, No. 2, 254–258.

Childs, D. W., Nolan, S. A., and Kilgore, J. J., 1990c, "Additional Test Results for Round-Hole-Pattern Damper Seals: Leakage, Friction Factors and Rotordynamic Force Coefficients," *ASME Journal of Tribology*, Vol. 112, No. 2, 365–371.

Childs, D. W., Baskharone, E., and Ramsey, C., 1991, "Test Results for Rotordynamic Coefficients of the SSME HPOTP (High-Pressure Oxygen Turbopump) Turbine Interstage Seal With Two Swirl Brakes," *Transactions of the ASME Journal of Tribology*, Vol. 113, No. 3, 577–583.

Conner, K. and Childs, D. W., 1993, "Rotordynamic Coefficients Test Results for a 4-Stage Brush Seal," *AIAA* Paper No. 90-2139.

Darden, J. M., Earhart, E. M., and Flowers, G. T., 1999, "Experimental Rotordynamic Characterization of Annular Seals: Facility and Methodology," *ASME Journal of Engineering for Gas Turbines and Power*, Vol. 121, 349–354.

Darden, J. M., Earhart, E. M., and Flowers, G. T., 2001, "Comparison of the Dynamic Characteristics of Smooth Annular Seals and Damping Seals," *ASME Journal of Engineering for Gas Turbines and Power*, Vol. 123, No. 4, 857–863.

Dawson, M. P. and Childs, D. W., 2002, "Measurements Versus Predictions for the Dynamic Impedances of Annular Gas Seals: Part 2 – Smooth and Honeycomb Geometries," *ASME Journal of Engineering for Gas Turbines and Power*, Vol. 124, No. 4, 963–970.

Dawson, M. P., Childs, D. W., Holt, C., and Phillips, S., 2002, "Measurements Versus Predictions for the Dynamic Impedances of Annular Gas Seals: Part 1 – Test Facility and Apparatus," *ASME Journal of Engineering for Gas Turbines and Power*, Vol. 124, No. 4, 958–963.

Dietzen, F. J. and Nordmann, R., 1987, "Calculating Rotordynamic Coefficients of Seals by Finite-Difference Techniques," *ASME Journal of Tribology*, Vol. 109, No. 3, 388–394.

D'Souza, R. and Childs, D., 2002, "A Comparison of Rotordynamic Coefficient Predictions of Annular Honeycomb Gas Seals Using Different Friction-Factor Models," *ASME Journal of Tribology,* Vol. 124, 524–529.

Elrod, H. G. Jr and Ng, C. W., 1967, "A Theory for Turbulent Fluid Films and its Application to Bearings," *ASME Journal of Lubrication Technology*, Vol. 89, No.3, 346–363.

Elrod, D., Nelson, C., and Childs, D., 1989, "An Entrance Region Friction Factor Model Applied to Annular Seal Analysis: Theory Versus Experiment for Smooth and Honeycomb Seals," *ASME Journal of Tribology*, Vol. 111, No. 2, 337–343.

Elrod. D., Childs, D., and Nelson, C., 1990, "An Annular Gas Seal Analysis Using Empirical Entrance and Exit Region Friction Factors," *ASME Journal of Tribology*, Vol. 112, 196–204.

Etison, I., 1982, "A Review of Mechanical Face Seal Dynamics," *Shock and Vibration and Digest*, Vol. 14, No. 2, 9–14.

Etison, I., 1985, "Mechanical Face Seal Dynamics Update," *Shock and Vibration and Digest*, Vol. 17, No. 4, 11–15.

Falco, M., Mimmi, G., Pizzigoni, B., Marenco, G., and Negri, G., 1984, "Plain Seal Dynamic Behaviour – Experimental and Analytical Results," in Proceedings of the 3rd International Conference on Vibration in Rotating Machinery, IMechE, York, UK, Paper No. C303, 151–158.

Flack, R. D. and Allaire, P. E., 1984a, "Lateral Forces on Pump Impellers: A Literature Review," *Shock and Vibration Digest*, Vol. 16, No. 1, 5–14.

Flack, R. D. and Allaire, P. E., 1984b, "Literature Review of Tilting Pad and Turbulent Hydrostatic Journal Bearings for Nuclear Main Coolant Pumps," *Shock and Vibration Digest*, Vol. 16, No. 7, 3–12.

Fleming, D. F., 1980, "Damping in Seals for Compressible Fluids," in Proceedings of the Workshop on Rotordynamic Instability Problems in High Performance Turbomachinery, Texas A&M University, NASA CP-2133.

Guo, Z. and Kirk, R. G., 2005, "CFD Evaluation of Turbomachinery Secondary Flow Leak Path and Labyrinth Seal Entry Swirl," in Proceedings of the 3rd International Symposium on Stability Control of Rotating Machinery, Cleveland, OH, September 19–23.

Ha, T.W. and Childs, D. W., 1992, "Friction-Factor Data for Flat-Plate Tests of Smooth and Honeycomb Surfaces," *ASME Journal of Tribology*, Vol. 14, 722–730.

Ha, T.-W. and Childs, D., 1994, "Annular Honeycomb-Stator Turbulent Gas Seal Analysis Using A New Friction-Factor Model Based on Flat Plate Tests," *ASME Journal of Tribology*, Vol. 116, 352–360.

Hawkins, L., Childs, D., and Hale, K., 1989, "Experimental Results for Labyrinth Gas Seals with Honeycomb Stators: Comparisons to Smooth-Stator Seals and Theoretical Prediction," *ASME Journal of Tribology*, Vol. 111, No. 1, 161–168.

Hirs, G. G., 1973, "A Bulk-Flow Theory for Turbulence in Lubricant Films," *ASME Journal of Lubrication Technology*, No. 2, 137–146.

Holman, J. P., 1978, *Experimental Methods for Engineers*, McGraw-Hill, New York, 45.

Holt, G. C. and Childs, D. W., 2002, "Theory Versus Experiment for the Rotordynamic Impedances of Two Hole-Pattern-Stator Gas Annular Seals," *ASME Journal of Tribology*, Vol. 124, No. 1, 137–143.

Ismail, M. and Brown, R. D., 1996, "Dynamic Coefficients of Long Annular Pump Seals – Further Experimental Results," in Proceedings of the 6th International Conference on Vibration in Rotating Machinery, IMechE, No. C500/060/96, 41–51.

Ismail, M. and Brown, R. D., 1998, "Estimation of the Dynamic Characteristics of Long Annular Seals using a Time Domain Technique," *ASME Journal of Vibration and Acoustics*, Vol. 120, No. 3, 705–712.

Iwatsubo, T., Motooka, N., and Kawai, R., 1982, "Flow Induced Force of Labyrinth Seal," in Proceedings of Second Workshop on Rotordynamic Instability Problems in High Performance Turbomachinery, Texas A&M University, May 10–12, NASA CP 2250, 205–222.

Iwatsubo, T., Sheng, B. C., and Ono, M., 1990, "An Experimental Study on the Static and Dynamic Characteristics of Damper Seals," in Proceedings of the 3rd International Conference on Rotordynamics, IFToMM, Lyons, France, 307–312.

Iwatsubo, T., Mochida, H., and Maysuda, M., 2005, "Static and Dynamic Data Labyrinth Seal for Optimum Design," in Proceedings of the 3rd International Symposium on Stability Control of Rotating Machinery, Cleveland, OH, September 19–23.

Kaneko, S., Kamei, H., Yanagisawa, Y., and Kawahara, H., 1998, "Experimental Study on Static and Dynamic Characteristics of Annular Plain Seals with Porous Materials," *ASME Journal of Tribology*, Vol. 120, No. 2, 165–172.

Kaneko, S., Ikeda, T., Saito, T., and Ito, S., 2003, "Experimental Study on Static and Dynamic Characteristics of Liquid Annular Convergent-Tapered Damper Seals with Honeycomb Roughness Pattern," *ASME Journal of Tribology*, Vol. 125, No. 3, 592–599.

Kanemori, Y. and Iwatsubo, T., 1992, "Experimental Study of Dynamic Fluid Forces and Moments for a Long Annular Seal," *Machinery Dynamics – Applications and Vibration Control Problems*, DE-Vol. 18-2, 141–148.

Kanki, H. and Kawakami, T., 1984, "Experimental Study on the Dynamic Characteristics of Pump Annular Seals," in Proceedings of the 3rd International Conference on Vibration in Rotating Machinery, IMechE, York, UK, Paper No. C297, 159–166.

Kim, C. H. and Childs, D. W., 1987, "Analysis for Rotordynamic Coefficients of Helically Grooved Turbulent Annular Seals," *ASME Journal of Tribology*, Vol. 109, No. 1, 136–143.

Kim, C. H. and Lee, Y. B., 1994, "Test Results for Rotordynamic Coefficients of Anti-Swirl Self-Injection Seals," *ASME Journal of Tribology*, Vol. 116, No. 3, 508–513.

Kirk, R. G., 1985, "Evaluation of Aerodynamic Instability Mechanisms for Centrifugal Compressors," ASME 85-DET-147.

Kirk, R. G., 1986, "Oil Seal Dynamics: Considerations for Analysis of Centrifugal Compressors," in Proceedings of the 15th Texas A&M Turbomachinery Symposium, Corpus Christi, TX.

Kirk, R. G., 1988, "Transient Response of Floating Ring Liquid Seals," *ASME Journal of Tribology*, Vol. 110, No. 3, 572–578.

Kirk, R. G., 1990, "A Method for Calculating Labyrinth Seal Inlet Swirl Velocity," *ASME Journal of Vibration and Acoustics*, Vol. 112, No. 3, 380–383.

Kirk, R. G. and Baheti, S. K., 1997, "Design of Liquid Seals for Centrifugal Compressors," in Proceedings of ASME Design Engineering Technical Conferences, Sacramento, CA.

Kirk, R. G. and Miller, W. H., 1977, "The Influence of High Pressure Oil Seals on Turbo-Rotor Stability," in ASLE/ASME Lubrication Conference, Kansas City, MO, October 3–5.

Kleynhans, G. and Childs, D., 1997, "The Acoustic Influence of Cell Depth on the Rotordynamic Characteristics of Smooth-Rotor/Honeycomb-Stator AnnularGas Seals," *ASME Journal of Engineering for Gas Turbines and Power*, Vol. 4, 949–957.

Krämer E., 1993, *Dynamics of Rotors and Foundations*, Springer-Verlag, New York.

Kurtin, K. A., Childs, D. W., San Andrés, L., and Hale, R. K., 1993, "Experimental Versus Theoretical Characteristics of a High-Speed Hybrid (Combination Hydrostatic and Hydrodynamic) Bearing," *ASME Journal of Tribology*, Vol. 115, 160–169.

Kwanka, K., 2000, "Dynamic Coefficients of Stepped Labyrinth Gas Seals," *ASME Journal of Engineering for Gas Turbines and Power*, Vol. 122, No. 3, 473–477.

Kwanka, K., 2001, "Improving the Stability of Labyrinth Gas Seals," *ASME Journal of Engineering for Gas Turbines and Power*, Vol. 123, No. 2, 383–387.

Laos, H. E., Vance, J. M., and Buchanan, S. E., 2000, "Hybrid Brush Pocket Damper Seals for Turbomachinery," *ASME Journal of Engineering for Gas Turbines and Power*, Vol. 122, No. 2, 330–336.

Li, J., San Andrés, L., and Vance, J., 1999a, "A Bulk-Flow Analysis of Multiple Pocket Gas Damper Seals," *ASME Journal of Gas Turbines and Power*, Vol. 121, No. 2, 355–362.

Li, J., Ransom, D., San Andrés, L., and Vance, J., 1999b, "Comparison of Predictions with Test Results for Rotordynamic Coefficients of a Four-Pocket Gas Damper Seal," *ASME Journal of Tribology*, Vol. 121, No. 2, 363–369.

Li, J., Aguilar, R., San Andrés, L., and Vance, J., 2000, "Dynamic Force Coefficients of a Multiple-Blade, Multiple-Pocket Gas Damper Seal: Test Results and Predictions," *ASME Journal of Tribology*, Vol. 122, No. 1, 317–322.

Lindsey, W. T. and Childs, D. W., 2000, "The Effects of Converging and Diverging Axial Taper on the Rotordynamic Coefficients of Annular Pressure Seals: Theory Versus Experiment," *ASME Journal of Vibration and Acoustics*, Vol. 122, No. 2, 126–131.

Lomakin, A. A., 1958, "Calculation of Critical Speed and Securing of Dynamic Stability of the Rotor of Hydraulic High Pressure Machines with Reference to Forces Arising in the Seal Gaps," *Energomashinostroenie*, Vol. 4, No. 4, 1–5 (in Russian).

Marquette, O. R. and Childs, D. W., 1997, "Theory Versus Experiment for Leakage and Rotordynamic Coefficients of Circumferentially Grooved Liquid Annular Seals With L/D of 0.45," FEDSM97-3333.

Marquette, O. R., Childs, D. W., and San Andrés, L., 1997, "Eccentricity Effects on the Rotordynamic Coefficients of Plain Annular Seals: Theory Versus Experiment," *ASME Journal of Tribology*, Vol. 119, No. 3, 443–448.

Moore, J. J., 2003, "Three-Dimensional CFD Rotordynamic Analysis of Gas Labyrinth Seals," *Journal of Vibration and Acoustics,* Vol. 125, No. 4, 427–433.

Murphy, B. T. and Vance, J. M., 1980, "Labyrinth Seal Effect on Rotor Whirl Stability," in Proceedings of the 2nd International Conference on Vibration in Rotating Machinery (Institution of Mechanical Engineering), Churchill College, Cambridge University, UK, September 1–4, Paper No. C306/80, 369–372.

Nakamura, R. and Iwatsubo, T., 2005, "Stabilization of Labyrinth Seal Force by Injecting the Leakage Flow to Preswirl Groove," in Proceedings of the 3rd International Symposium on Stability Control of Rotating Machinery, Cleveland, OH, September 19–23.

Nelson, C. C., 1984, "Analysis for Leakage and Rotordynamic Coefficients of Surface Roughened Tapered Annular Gas Seals," *ASME Journal of Engineering for Power,* Vol. 106, No. 4, 927–934.

Nelson, C. and Nguyen, D., 1987, "Comparison of Hirs' Equation with Moody's Equation for Determining Rotordynamic Coefficients of Annular Pressure Seals," *ASME Journal of Tribology*, Vol. 109, No. 3, 144–148.

Nelson, C. C., Childs, D. W., Nicks, C., and Elrod, D., 1986, "Theory Versus Experimental for the Rotordynamic Coefficients of Annular Gas Seals: Part II: Constant-Clearance and Convergent-Tapered Geometry," *ASME Journal of Tribology*, Vol. 108, No. 3, 433–438.

Ng, C. W. and Pan, C. H. T., 1965, "A Linearized Turbulent Lubrication Theory," *ASME Journal of Basic Engineering*, Vol. 87, No. 3, 675–688.

Nielsen, K. K., Childs, D. W., and Myllerup, C. M., 2001, "Experimental and Theoretical Comparison of Two Swirl Brake Designs," *ASME Journal of Turbomachinery*, Vol. 123, No. 2, 353–358.

Nordmann, R. and Massmann, H., 1984, "Estimation of Stiffness, Damping and Mass Coefficients of Annular Seals," in Proceedings of the 3rd International Conference on Vibration in Rotating Machinery, IMechE, York, UK, Paper No. C280, 167–181.

Oike, M., Nosaka, M., Kikuchi, M., and Hasegawa, S., 1999, "Two-Phase Flow in Floating-Ring Seals for Cryogenic Turbopumps," in ASME/STLE Tribology Conference, Toronto, Ontario, Canada.

Padavala, S., Palazzolo, A. B., Vallely, D. P., and Ryan, S. G., 1993, "Application of an Improved Nelson–Nguyen Analysis to Eccentric, Arbitrary Profile Liquid Annular Seals," in Workshop on Rotordynamic Instability Problems in High Performance Turbomachinery, Texas A&M University, 113–135.

Pelletti, J. M. and Childs, D. W., 1991, "A Comparison of Experimental Results and Theoretical Predictions for the Rotordynamic Coefficients of Short (*L/D*) Labyrinth Seals," in *ASME Design Technical Conference,* September, ASME-DE Vol. 35, 69–76.

Ransom, D., Li, J., San Andrés, L., and Vance, J. M., 1999, "Experimental Force Coefficients for a Two-Bladed Labyrinth Seal and a Four-Pocket Damper Seal," *ASME Journal of Tribology*, Vol. 121, No. 2, 370–376.

Rao, J. S., 2000, *Vibratory Condition Monitoring of Machines*, Narosa, New Delhi.

Reedy, S. W. and Kirk, R. G., 1992, "Advanced Analysis of Multi-Ring Liquid Seals," *ASME Journal of Vibration and Acoustics*, Vol. 114, No. 1, 42–46.

San Andrés, L., 1991, "Analysis of Variable Fluid Properties, Turbulent Annular Seals," *ASME Journal of Tribology*, Vol. 113, No. 4, 694–702.

Scharrer, J., 1988, "Theory Versus Experiment for the Rotordynamic Coefficients of Labyrinth Gas Seals: Part I – A Two Control Volume Model," *ASME Journal of Vibration, Acoustics, Stress, and Reliability in Design*, Vol. 110, No. 3, 270–280.

Scharrer, J. K. and Nelson, C. C., 1991a, "Rotordynamic Coefficients for Partially Tapered Annular Seals: Part I – Incompressible Flow," *ASME Journal of Tribology*, Vol. 113, 48–52.

Scharrer, J. K. and Nelson, C. C., 1991b, "Rotordynamic Coefficients for Partially Tapered Annular Seals: Part II – Compressible Flow," *ASME Journal of Tribology,* Vol. 113, 53–57.

Simon, F. and Frêne, J., 1989, "Static and Dynamic Characteristics of Turbulent Annular Eccentric Seals: Effect of Convergent-Tapered Geometry and Variable Fluid Properties," *ASME Journal of Tribology,* Vol. 111, 378–384.

Soto, E. A. and Childs, D. W., 1999, "Experimental Rotordynamic Coefficient Results for (a) a Labyrinth Seal With and Without Shunt Injection and (b) a Honeycomb Seal," *ASME Journal of Engineering for Gas Turbines and Power*, Vol. 121, No. 1, 153–159.

Suzuki, M., Nosaka, M., Kamijo, K., and Kikuchi, M., 1986, "Research and Development of a Rotating-Shaft Seal for a Liquid Hydrogen Turbopump," *Lubrication of Technology*, Vol. 42, No. 3, 162–169.

Swanson, E. E. and Kirk, R. G., 1997, "Survey of Experimental Data for Fixed Geometry Hydrodynamic Journal Bearings," *ASME Journal of Tribology*, Vol. 119, 704–710.

Tiwari, R., Lees, A. W., and Friswell, M. I., 2002, "Identification of Speed-Dependent Bearing Parameters," *Journal of Sound and Vibration*, Vol. 254, No. 5, 967–986.

Tiwari, R., Lees, A. W., and Friswell, M. I., 2004, "Identification of Dynamic Bearing Parameters: A Review," *Shock and Vibration Digest*, Vol. 36, No. 2, 99–124.

Vance, J. M., 1998, *Rotordynamics of Turbomachinery,* Wiley, New York.

Vance, J. M. and Li, J., 1996, "Test Results of a New Damper Seal for Vibration Reduction in Turbomachinery," *ASME Journal of Engineering for Gas Turbines and Power*, Vol. 118, No. 4, 843–846.

Vance, J. M. and Schultz, R. R., 1993, "A New Damper Seal for Turbomachinery," *Vibration of Rotating Systems, ASME* DE-Vol. 60, 139–148.

Wagner, N. G., 2001, "Reliable Rotor Dynamic Design of High-Pressure Compressors Based on Test Rig Data," *ASME Journal of Engineering for Gas Turbines and Power*, Vol. 123, 849–856.

Wagner, N. G. and Steff, K., 1996, "Dynamic Labyrinth Coefficients From a High-Pressure Full-Scale Test Rig Using Magnetic Bearings," *Rotordynamic Instability Problems in High-Performance Turbomachinery,* NASA Conf. Publ. 3344, 95–112.

Weatherwax, M. and Childs, D. W., 2003, "Theory Versus Experiment for the Rotordynamic Characteristics of a High Pressure Honeycomb Annular Gas Seal at Eccentric Positions," *ASME Journal of Tribology*, Vol. 125, No. 2, 422–429.

Wilkes, K. W., Kirk, R. G., and Elrod, D. A., 1993, "Rotordynamics Analysis of Circumferentially Grooved Turbulent Seals: Theory and Comparison to Published Test Results," *STLE Tribology Transactions*, Vol. 36, No. 2, 183–192.

Wright, D. V., 1978, "Air Model Test of Labyrinth Seal Forces on a Whirling Rotor," *ASME Journal of Engineering for Power*, Vol. 100, No. 4, 533–543.

Wright, D. V., 1983, "Labyrinth Seal Forces on a Whirling Rotor," *Rotor Dynamical Stability*, AMD-Vol. 55, 19–31.

Wyssmann, H. R., Pham, T. C., and Jenny, R. J., 1984, "Prediction of Stiffness and Damping Coefficients for Centrifugal Compressor Labyrinth Seals," *ASME Journal of. Engineering for Gas Turbines and Power*, Vol. 106, No. 1, 920–926.

Yang, Z., 1993, "Dynamic Force Performance of Annular Gas Seal at Center Conditions," *STLE* Paper 93-AM-4D-1.

Yücel, U., 2003, "Calculation of Leakage and Dynamic Coefficients of Stepped Labyrinth Gas Seals," *Applied Mathematics and Computation*, Vol. 152, 521–533.